Two-loop QCD helicity amplitudes for $q\overline{q} \to W \pm$ and $q\overline{q} \to Z\ 0$

Gehrmann, Thomas ; Tancredi, Lorenzo

Abstract: The self-couplings of the electroweak gauge bosons are probed at hadron colliders through the production of a massive gauge boson and a photon. To extend the theoretical description of this type of final states towards next-to-next-to-leading order (NNLO) in QCD, we derive the two-loop QCD corrections to the helicity amplitudes describing the production of a massive gauge boson in association with a real photon. Our results are obtained by applying projectors to the general parton-level tensor structure. The leptonic decay of the vector boson is included, thus allowing for a fully exclusive description of the final state. The infrared poles of the amplitudes are described by an infrared factorization formula. We provide an analytic expression for the finite remainder of the amplitude in terms of one- and two-dimensional harmonic polylogarithms. The amplitudes are expressed in the physical kinematics relevant to gauge-boson-plus-photon production at hadron colliders. As a by-product, we also derive the two-loop QCD amplitudes for vector-boson-plus-jet production at hadron colliders.

DOI: https://doi.org/10.1007/JHEP02(2012)004

Preprint typeset in JHEP style - PAPER VERSION ZU-TH 26/11

Two-loop QCD helicity amplitudes for $q\bar{q} \to W^{\pm}\gamma$ and $q\bar{q} \to Z^0\gamma$

Thomas Gehrmann, Lorenzo Tancredi

Institut für Theoretische Physik, Universität Zürich, Winthertur erstrasse 190, CH-8057 Zürich, Switzerland

Abstract: The self-couplings of the electroweak gauge bosons are probed at hadron colliders through the production of a massive gauge boson and a photon. To extend the theoretical description of this type of final states towards next-to-next-to-leading order (NNLO) in QCD, we derive the two-loop QCD corrections to the helicity amplitudes describing the production of a massive gauge boson in association with a real photon. Our results are obtained by applying projectors to the general parton-level tensor structure. The leptonic decay of the vector boson is included, thus allowing for a fully exclusive description of the final state. The infrared poles of the amplitudes are described by an infrared factorization formula. We provide an analytic expression for the finite remainder of the amplitude in terms of one- and two-dimensional harmonic polylogarithms. The amplitudes are expressed in the physical kinematics relevant to gauge-boson-plus-photon production at hadron colliders. As a by-product, we also derive the two-loop QCD amplitudes for vector-boson-plus-jet production at hadron colliders.

Keywords: QCD, Collider Physics, NLO and NNLO Calculations.

Contents

1. Introduction

Pair production of electroweak gauge bosons ($\gamma, W^{\pm}, Z^0$) offers a wide spectrum of observables, which allow to test the theory of the electroweak interaction, to probe the Higgs mechanism of electroweak symmetry breaking and to search for physics beyond the standard model. While photons are directly observed in the detector, the massive W and Z bosons are identified from their leptonic decay modes.

The standard model predicts specific values and structures for the couplings among the electroweak gauge bosons: $W^{\pm}$, Z^0 and γ. Physics effects beyond the standard model could modify these gauge boson self-couplings [1, 2]. Observations of such anomalous couplings may help to constrain new theory models and could provide indirect evidence for new physics effects at energy scales above the nominal collision energy. The couplings of the massive $W^{\pm}, Z^0$ bosons to the photon are determined at hadron colliders by measuring $W^{\pm}\gamma$ and $Z^0\gamma$ production cross sections and comparing them to theoretical predictions. Measurements have been carried out at Tevatron [3], and first results from the LHC are already becoming available [4]. The accuracy of the coupling determination is potentially limited by both the experimental accuracy and by uncertainties inherent to the theoretical prediction.

At present, $W^{\pm}\gamma$ and $Z^0\gamma$ production at hadron colliders is described theoretically to next-to-leading order (NLO) in QCD [2,5,6] and to NLO in the electroweak theory [7]. With

increasing order in perturbative QCD, new production channels (with new combinations of parton distributions) for vector boson pairs start contributing; the complete spectrum of partonic channels is only present from next-to-next-to-leading order (NNLO) onwards. Moreover, the inclusion of NNLO corrections to gauge boson pair production will lower the inherent theoretical uncertainty of the prediction (usually quantified by variation of the renormalisation and factorisation scales) and allow for a fully consistent inclusion of NNLO parton distribution functions.

The calculation of gauge boson pair production at NNLO requires three types of ingredients: the two-loop partonic $2 \to 2$ matrix elements for the production of the gauge boson pair under consideration, the one-loop partonic $2 \to 3$ matrix elements for the production of the gauge boson pair in association with an extra parton and the tree-level $2 \to 4$ matrix elements involving two extra partons. The latter two contributions are equally contributing to the NLO corrections for the production of a vector boson pair with an extra jet, which have been computed for $\gamma\gamma j$ [8], $V\gamma j$ [9] and VVj [10] already some time ago. At NNLO, the contributions from both these channels will contain infrared singularities from one or two final state partons becoming soft or collinear. These singularities cancel only when combined with the infrared-singular two-loop contributions, such that a method is needed for their extraction from the real radiation processes. Several methods have been applied successfully in NNLO calculations of exclusive observables in the recent past: sector decomposition [11], q_T-subtraction [12] and antenna subtraction [13–15]. It should be noted that the q_T-subtraction method is restricted to observables that are described by non-QCD processes at leading order, which is the case for vector boson pair production. The first calculation of NNLO corrections to a vector boson pair production process ($pp \to \gamma\gamma$) has been performed most recently [16] using this method.

The two-loop parton-level matrix elements for vector boson pair production are at present known only for $q\bar{q} \to \gamma\gamma$ [17] and $gg \to \gamma\gamma$ [18] (where the latter two-loop amplitude formally contributes only beyond NNLO). The high energy approximation for $q\bar{q} \to W^+W^-$ and $q\bar{q} \to Z^0Z^0$ has also been derived [19]. It is the purpose of this paper to compute the two-loop corrections to the matrix elements for the production of a massive vector boson and a photon: $q\bar{q} \to W^\pm\gamma$ and $q\bar{q} \to Z^0\gamma$. The calculation follows closely the techniques that were employed in the calculation of two-loop corrections to the $\gamma^* \to q\bar{q}g$ matrix elements [20,21], which were a crucial ingredient to the NNLO corrections [22,23] to three-jet production and related event shapes at e^+e^- colliders.

This paper is structured as follows: in Section 2, we fix the notation and discuss the basic helicity structure of the process under consideration. The calculation of the two-loop amplitudes is described in Section 3, and the results are discussed in Section 4. The two-loop helicity amplitudes are obtained in a closed analytic form, which is however too large to be quoted in the paper, and we enclose computer algebra files containing the results with the submission. We performed several non-trivial checks on the results, which are described in Section 5. We conclude with an outlook in Section 6. We enclose appendices with the one-loop helicity amplitudes, examples of selected colour coefficients in the two-loop amplitudes and with a discussion on kinematical crossings, including the two-loop matrix elements relevant to vector-boson-plus-jet production: $q\bar{q} \to Vg$ and $qg \to Vq$.

2. Kinematics and basic helicity structure

The production of a massive vector boson and a photon in quark-antiquark annihilation is related by crossing to the decay of the vector boson into a quark-antiquark-photon final state, which has the same kinematics as three-jet-production ($3j$) in e^+e^- annihilation. Technically, the calculation of QCD corrections to the $q\bar{q} \to V\gamma$ amplitudes is thus similar to previous calculations for the helicity amplitudes for $3j$-production, which have been derived to two-loop accuracy in QCD [21].

Including the leptonic decay of the vector boson, the partonic subprocesses yielding $V\gamma$ final states are:

$$\begin{aligned}
&q(p_2) + \bar{q}(p_1) \to \gamma(-p_3) + Z^0(q) \to \gamma(-p_3) + l^+(p_5) + l^-(p_6) \,, \\
&q(p_2) + \bar{q}'(p_1) \to \gamma(-p_3) + W^-(q) \to \gamma(-p_3) + \bar{\nu}(p_5) + l^-(p_6) \,, \\
&q(p_2) + \bar{q}'(p_1) \to \gamma(-p_3) + W^+(q) \to \gamma(-p_3) + l^+(p_5) + \nu(p_6) \,.
\end{aligned}$$

The Z^0-boson process implicitly includes also a contribution from an off-shell photon γ^*. In the most general case where two quarks of two different flavours appear, to fix the conventions, we will refer from now on to p_1 as the momentum of the anti-quark $\bar{q}'$ and as p_2 to the momentum of the quark q. The momentum of the vector boson is given by

$$q^\mu = p_5^\mu + p_6^\mu \,. \tag{2.1}$$

It is convenient to define the invariants

$$s_{12} = (p_1 + p_2)^2 \,, \qquad s_{13} = (p_1 + p_3)^2 \,, \qquad s_{23} = (p_2 + p_3)^2 \,, \tag{2.2}$$

which fulfil

$$q^2 = (p_1 + p_2 + p_3)^2 = s_{12} + s_{13} + s_{23} \equiv s_{123} \,, \tag{2.3}$$

as well as the dimensionless invariants

$$x = s_{12}/s_{123} \,, \qquad y = s_{13}/s_{123} \,, \qquad z = s_{23}/s_{123} \,, \tag{2.4}$$

which satisfy $x + y + z = 1$.

In $3j$-production, q^2 is time-like (hence positive) and all the s_{ij} are also positive, which implies that x, y, z all lie in the interval $[0; 1]$, with the above constraint $x + y + z = 1$. For the $V\gamma$ production, q^2 remains time-like, but only s_{12} is positive:

$$q^2 > 0 \,, \quad s_{12} > 0 \,, \quad s_{13} < 0, \quad s_{23} < 0 \,, \tag{2.5}$$

or, equivalently,

$$x > 0 \,, \quad y < 0 \,, \quad z < 0 \,. \tag{2.6}$$

It was shown in [24] that the kinematical situation of this configuration can be expressed by introducing new dimensionless variables

$$u = -\frac{s_{13}}{s_{12}} = -\frac{y}{x} \,, \qquad v = \frac{q^2}{s_{12}} = \frac{1}{x} \,, \tag{2.7}$$

which fulfil

$$0 \leq u \leq v\,, \qquad 0 \leq v \leq 1\,.$$

The helicity amplitudes for $q\bar{q} \to V\gamma$ can be expressed as a product of a partonic current S_μ and a leptonic current L_μ:

$$A(p_5, p_6; p_1, p_3, p_2) = L^\mu(p_5; p_6) S_\mu(p_1; p_3; p_2)\,. \tag{2.8}$$

Only the partonic current receives contributions from QCD radiative corrections, and it can be perturbatively decomposed as:

$$\begin{aligned} S_\mu(p_1; p_3; p_2) = \sqrt{4\pi\alpha}\,\Big(& S_\mu^{(0)}(p_1; p_3; p_2) + \left(\frac{\alpha_s}{2\pi}\right) S_\mu^{(1)}(p_1; p_3; p_2) \\ & + \left(\frac{\alpha_s}{2\pi}\right)^2 S_\mu^{(2)}(p_1; p_3; p_2) + \mathcal{O}(\alpha_s^3)\Big). \end{aligned} \tag{2.9}$$

It is a colour-singlet. The vector boson decay to a lepton-antilepton pair is described by a leptonic current. To be as general as possible, we consider only the basic amplitude structure in the partonic and leptonic current, and include charges and coupling factors related to the massive vector boson only when assembling the final results. We have extracted a factor $e = \sqrt{4\pi\alpha}$ for the photon coupling in the partonic current, such that all the quark charges will be expressed in units of e.

The most general structure of the partonic current can be derived from symmetry considerations [21]:

$$\begin{aligned} S_\mu(p_1; p_3; p_2) = & A_{11}\, T_{11\mu} + A_{12}\, T_{12\mu} + A_{13}\, T_{13\mu} \\ & + A_{21}\, T_{21\mu} + A_{22}\, T_{22\mu} + A_{23}\, T_{23\mu} \\ & + B\, T_\mu\,, \end{aligned} \tag{2.10}$$

where $T_{ij\mu}$ and T_μ are the following tensor structures:

$$\begin{aligned} T_{1j\mu} &= \bar{v}(p_1)\left[\not{p}_3\, \epsilon_3 \cdot p_1\, p_{j\mu} - \frac{s_{13}}{2}\not{\epsilon}_3\, p_{j\mu} + \frac{s_{j4}}{4}\not{\epsilon}_3\not{p}_3\gamma_\mu\right] u(p_2), \\ T_{2j\mu} &= \bar{v}(p_1)\left[\not{p}_3\, \epsilon_3 \cdot p_2\, p_{j\mu} - \frac{s_{23}}{2}\not{\epsilon}_3\, p_{j\mu} + \frac{s_{j4}}{4}\gamma_\mu\not{p}_3\not{\epsilon}_3\right] u(p_2), \\ T_\mu &= \bar{v}(p_1)\left[s_{23}\left(\gamma_\mu \epsilon_3 \cdot p_1 + \frac{1}{2}\not{\epsilon}_3\not{p}_3\gamma_\mu\right) - s_{13}\left(\gamma_\mu \epsilon_3 \cdot p_2 + \frac{1}{2}\gamma_\mu\not{p}_3\not{\epsilon}_3\right)\right] u(p_2), \end{aligned} \tag{2.11}$$

where we defined:

$$s_{14} = s_{12} + s_{13}, \quad s_{24} = s_{12} + s_{23}, \quad s_{34} = s_{13} + s_{23}.$$

The tensor coefficients A_{ij} and B can be determined by appropriate projectors, applied to the Feynman-diagrammatic expression of the amplitude. Projections on the diagrams are performed in dimensional regularisation in $d = 4 - 2\epsilon$ dimensions. The projectors can be found in [21].

Each of the unrenormalised coefficients A_{ij} and B has a perturbative expansion of the form

$$A_{ij}^{\rm un} = \sqrt{4\pi\alpha}\left[A_{ij}^{(0),{\rm un}} + \left(\frac{\alpha_s}{2\pi}\right) A_{ij}^{(1),{\rm un}} + \left(\frac{\alpha_s}{2\pi}\right)^2 A_{ij}^{(2),{\rm un}} + \mathcal{O}(\alpha_s^3)\right]\,,$$

$$B^{\rm un} = \sqrt{4\pi\alpha}\,\left[B^{(0),{\rm un}} + \left(\frac{\alpha_s}{2\pi}\right) B^{(1),{\rm un}} + \left(\frac{\alpha_s}{2\pi}\right)^2 B^{(2),{\rm un}} + \mathcal{O}(\alpha_s^3)\right], \tag{2.12}$$

where the dependence on $(s_{13}, s_{23}, s_{123})$ is implicit.

By fixing the helicities of the partons, the partonic current can be cast in the usual spinor helicity notation [25]. All helicity configurations can be obtained from the amplitude

$$\begin{aligned} S^\mu_R(p_1^-;p_3^+;p_2^+) &= \frac{1}{\sqrt{2}}\langle 12\rangle[13]^2\,(p_{1\mu}A_{11} + p_{2\mu}A_{12} + p_{3\mu}A_{13}) - \frac{1}{\sqrt{2}}\frac{\langle 12\rangle[13]}{\langle 23\rangle}[1\,|\gamma_\mu|\,2\rangle\; s_{23}B \\ &+ \frac{1}{\sqrt{2}}[13][3\,|\gamma_\mu|\,2\rangle\;\left[s_{23}B + \frac{1}{2}\left((A_{11}+A_{12})s_{12} + (A_{11}+A_{13})s_{13} + (A_{12}+A_{13})s_{23}\right)\right] \end{aligned} \tag{2.13}$$

by charge and parity conversion. For $\bar{q}'(p_1)$, $q(p_2)$ incoming, the above amplitude corresponds to a right-handed current. Notice that (2.13) has been obtained assuming that the momentum of the photon is $-p_3$. We have:

$$\begin{aligned} S^\mu_L(p_1^+;p_3^-;p_2^-) &= \left[S^\mu_R(p_1^-;p_3^+;p_2^+)\right]^*, \\ S^\mu_L(p_1^+;p_3^+;p_2^-) &= -S^\mu_R(p_2^-;p_3^+;p_1^+), \\ S^\mu_R(p_1^-;p_3^-;p_2^+) &= \left[-S^\mu_R(p_2^-;p_3^+;p_1^+)\right]^*. \end{aligned} \tag{2.14}$$

It is also straightforward to include the spin-correlations with the leptonic decay products by contracting the partonic current with the leptonic current L_μ for fixed helicities of the final state leptons. Consider the decay of the vector boson V into two leptons:

$$V(q) \longrightarrow l^+(p_5) + l^-(p_6).$$

The purely vectorial tree-level leptonic current reads:

$$L^\mu(p_5,p_6) = \bar{u}(p_6)\,\gamma^\mu\,v(p_5), \tag{2.15}$$

where in the case of an outgoing lepton-antilepton pair $L_\mu(p_5^-,p_6^+)$ corresponds to a right handed current, and $L_\mu(p_5^+,p_6^-)$ to a left-handed current. We find straightforwardly:

$$L^\mu_R(p_5^-,p_6^+) = [6\,|\gamma^\mu|\,5\rangle, \qquad L^\mu_L(p_5^+,p_6^-) = [5\,|\gamma^\mu|\,6\rangle = [L^\mu_R(p_5^-,p_6^+)]^*. \tag{2.16}$$

In order to write down the lepton-parton contraction it is convenient to introduce the set of helicity coefficients defined in [21]:

$$\alpha(u,v) = \frac{s_{13}s_{23}}{4}\Big(2B + A_{12} - A_{11}\Big), \tag{2.17}$$

$$\beta(u,v) = \frac{s_{13}}{4}\Big(2s_{23}B + 2(s_{12}+s_{13})A_{11} + s_{23}(A_{12}+A_{13})\Big), \tag{2.18}$$

$$\gamma(u,v) = \frac{s_{13}s_{23}}{4}\Big(A_{11} - A_{13}\Big), \tag{2.19}$$

$$\delta(u,v) = -\frac{s_{12}s_{13}}{4}A_{11}, \tag{2.20}$$

which, from their definition in terms of the coefficients A_{ij} and B, respect the relation

$$\alpha(u,v) - \beta(u,v) - \gamma(u,v) - \frac{2s_{123}}{s_{12}}\delta(u,v) = 0. \tag{2.21}$$

The relations above can be inverted for A_{11}, $A_{12}+2B$ and A_{13}, and in these variables the contracted amplitude assumes a particularly simple form. We take the contraction of the right-handed quark current with positive photon helicity, and the right-handed leptonic current, as basic object from which all other helicity configurations are obtained:

$$\begin{aligned} &A^+_{RR}(p_5,p_6;p_1,p_3,p_2) = L^\mu_R(p_5^-;p_6^+)S_{R,\mu}(p_1^-;p_3^+;p_2^+) \\ &= -2\sqrt{2}\left[\frac{\langle 25\rangle\langle 12\rangle[16]}{\langle 13\rangle\langle 23\rangle}\,\alpha(u,v) - \frac{\langle 25\rangle[36]}{\langle 13\rangle}\,\beta(u,v) + \frac{\langle 15\rangle[13][36]}{\langle 13\rangle[23]}\,\gamma(u,v)\right]. \end{aligned} \tag{2.22}$$

The unrenormalised helicity amplitude coefficients α, β and γ are vectors in colour space and have perturbative expansions:

$$\Omega^{\rm un} = \sqrt{4\pi\alpha}\,\delta_{ij}\left[\Omega^{(0),{\rm un}} + \left(\frac{\alpha_s}{2\pi}\right)\Omega^{(1),{\rm un}} + \left(\frac{\alpha_s}{2\pi}\right)^2\Omega^{(2),{\rm un}} + \mathcal{O}(\alpha_s^3)\right], \tag{2.23}$$

for $\Omega = \alpha, \beta, \gamma$. The dependence on (u,v) is again implicit.

From $A^+_{RR}(p_5,p_6;p_1,p_3,p_2)$, all other helicity amplitudes can be obtained by parity and charge conjugation. Axial contributions from the weak gauge boson couplings can be accounted for in a straightforward manner, by simply reweighting the different right-handed and left-handed helicity amplitudes with appropriate weights.

The eight possible helicity configurations are obtained from A^+_{RR} as follows:

$$\begin{aligned} &L^\mu_R(p_5^-;p_6^+)S_{R\mu}(p_1^-;p_3^+;p_2^+) = A^+_{RR}(p_5,p_6;p_1,p_3,p_2), \\ &L^\mu_R(p_5^-;p_6^+)S_{R\mu}(p_1^-;p_3^-;p_2^+) = A^-_{RR}(p_5,p_6;p_1,p_3,p_2) = [-A^+_{RR}(p_6,p_5;p_2,p_3,p_1)]^*, \\ &L^\mu_R(p_5^-;p_6^+)S_{L\mu}(p_1^+;p_3^+;p_2^-) = A^+_{RL}(p_5,p_6;p_1,p_3,p_2) = -A^+_{RR}(p_5,p_6;p_2,p_3,p_1), \\ &L^\mu_R(p_5^-;p_6^+)S_{L\mu}(p_1^+;p_3^-;p_2^-) = A^-_{RL}(p_5,p_6;p_1,p_3,p_2) = [A^+_{RR}(p_6,p_5;p_1,p_3,p_2)]^*, \end{aligned} \tag{2.24}$$

$$\begin{aligned} &L^\mu_L(p_5^+;p_6^-)S_{R\mu}(p_1^-;p_3^+;p_2^+) = A^+_{LR}(p_5,p_6;p_1,p_3,p_2) = A^+_{RR}(p_6,p_5;p_1,p_3,p_2), \\ &L^\mu_L(p_5^+;p_6^-)S_{R\mu}(p_1^-;p_3^-;p_2^+) = A^-_{LR}(p_5,p_6;p_1,p_3,p_2) = [-A^+_{RR}(p_5,p_6;p_2,p_3,p_1)]^*, \\ &L^\mu_L(p_5^+;p_6^-)S_{L\mu}(p_1^+;p_3^+;p_2^-) = A^+_{LL}(p_5,p_6;p_1,p_3,p_2) = -A^+_{RR}(p_6,p_5;p_2,p_3,p_1), \\ &L^\mu_L(p_5^+;p_6^-)S_{L\mu}(p_1^+;p_3^-;p_2^-) = A^-_{LL}(p_5,p_6;p_1,p_3,p_2) = [A^+_{RR}(p_5,p_6;p_1,p_3,p_2)]^*. \end{aligned} \tag{2.25}$$

The general form of the gauge boson coupling to fermions is:

$$\mathcal{V}^{V,f_1f_2}_\mu = -i\,e\,\Gamma^{V,f_1f_2}_\mu \qquad \text{with} \qquad e = \sqrt{4\pi\alpha}, \tag{2.26}$$

whose explicit form depends on the gauge boson, on the type of fermions, and on their helicities:

$$\Gamma^{V,f_1f_2}_\mu = L^V_{f_1f_2}\,\gamma_\mu\left(\frac{1-\gamma_5}{2}\right) + R^V_{f_1f_2}\,\gamma_\mu\left(\frac{1+\gamma_5}{2}\right). \tag{2.27}$$

The left- and right-handed couplings are identical for a pure vector interaction, and are in general different if vector and axial-vector interactions contribute. Their values for a photon are

$$L^{\gamma}_{f_1 f_2} = R^{\gamma}_{f_1 f_2} = -e_{f_1}\,\delta_{f_1 f_2}, \tag{2.28}$$

while for a Z boson

$$L^{Z}_{f_1 f_2} = \frac{I_3^{f_1} - \sin^2\theta_w e_{f_1}}{\sin\theta_w \cos\theta_w}\,\delta_{f_1 f_2}\ , \qquad R^{Z}_{f_1 f_2} = -\frac{\sin\theta_w e_{f_1}}{\cos\theta_w}\,\delta_{f_1 f_2}\ , \tag{2.29}$$

and finally for a $W^{\pm}$

$$L^{W}_{f_1 f_2} = \frac{1}{\sqrt{2}\,\sin\theta_w}\ , \qquad R^{W}_{f_1 f_2} = 0. \tag{2.30}$$

The charges e_i are measured in units of the fundamental electric charge $e > 0$.

The vector boson propagator can be written as:

$$P^{V}_{\mu\nu}(q,\xi) = \frac{i\,\Delta^{V}_{\mu\nu}(q,\xi)}{D_V(q)}, \tag{2.31}$$

where $\Delta^{V}_{\mu\nu}(q,\xi)$ and $D_V(q)$ are, respectively, the numerator and the denominator in the R_ξ gauge:

$$\Delta^{V}_{\mu\nu}(q,\xi) = \left(-g_{\mu\nu} + (1-\xi)\frac{q_\mu q_\nu}{q^2 - \xi M_V^2}\right), \tag{2.32}$$

$$D_{Z,W^{\pm}}(q) = \left(\, q^2 - M_V^2 + i\Gamma_V M_V \,\right), \tag{2.33}$$

$$D_{\gamma}(q) = q^2. \tag{2.34}$$

In the narrow-width approximation we can simplify expression (2.33) to

$$D_{Z,W^{\pm}}(q) \approx i\Gamma_V M_V \qquad \text{and} \qquad q^2 = M_V^2, \tag{2.35}$$

where M_V is the mass of the vector boson, while Γ_V is its decay width.

Since we do not consider any electroweak corrections, the vector boson V is always coupled to a fermion line and this allows us to neglect the R_ξ dependence (or equivalently to put $\xi = 1$). With this notation we obtain for the different choices of $V = (\gamma^*, Z, W^{\pm})$, and helicity combinations (with the obvious notation $p_{ij} = p_i + p_j$):

$$\mathcal{M}_V(p_5^-, p_6^+; p_1^-, p_3^+, p_2^+) = -i\,(4\pi\alpha)\,\frac{R^{V}_{q_1 q_2}\,R^{V}_{f_5 f_6}}{D_V(p_{56})}\,A^{+}_{RR}(p_5, p_6; p_1, p_3, p_2), \tag{2.36}$$

$$\mathcal{M}_V(p_5^-, p_6^+; p_1^+, p_3^-, p_2^-) = -i\,(4\pi\alpha)\,\frac{L^{V}_{q_1 q_2}\,R^{V}_{f_5 f_6}}{D_V(p_{56})}\,[A^{+}_{RR}(p_6, p_5; p_1, p_3, p_2)]^*, \tag{2.37}$$

$$\mathcal{M}_V(p_5^-, p_6^+; p_1^+, p_3^+, p_2^-) = -i\,(4\pi\alpha)\,\frac{L^{V}_{q_1 q_2}\,R^{V}_{f_5 f_6}}{D_V(p_{56})}\,[-A^{+}_{RR}(p_5, p_6; p_2, p_3, p_1)], \tag{2.38}$$

$$\mathcal{M}_V(p_5^-, p_6^+; p_1^-, p_3^-, p_2^+) = -i\,(4\pi\alpha)\,\frac{R^{V}_{q_1 q_2}\,R^{V}_{f_5 f_6}}{D_V(p_{56})}\,[-A^{+}_{RR}(p_6, p_5; p_2, p_3, p_1)]^*. \tag{2.39}$$

The corresponding amplitudes for left-handed leptonic current can be obtained simply interchanging $p_5 \leftrightarrow p_6$ and $R^{V}_{f_5 f_6} \to L^{V}_{f_5 f_6}$.

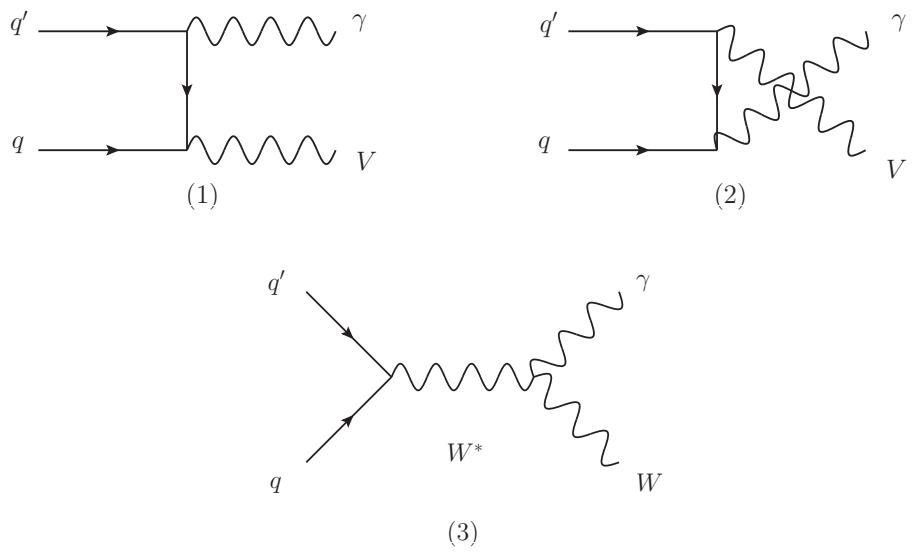

Figure 1: Abelian and non-abelian tree-level contribution.

3. Outline of the calculation

The two-loop corrections to the coefficients Ω for $W^{\pm}\gamma$ and $Z^0\gamma$ production can be evaluated through a calculation of the relevant Feynman diagrams. The diagrams which contribute at the two-loop level can be organised in different classes, some of which are present in both $V = Z^0, W^{\pm}$ cases, while others contribute only to one of the two processes.

To identify the different classes of diagrams, it is useful to start with the tree-level. We can define three classes of processes, each represented by a single diagram:

1. We call $I_1^{(0)}$ the contribution from diagram (1) in Figure 1, where the photon is attached on the quark q'. The charge factor of this diagram is $e_{q'}$.

2. We refer as $I_2^{(0)}$ to the contribution from diagram (2) in Figure 1, where the photon is attached on the quark q. The charge factor of this diagram is e_q.

3. $I_3^{(0)}$ is finally the contribution from diagram (3) in Figure 1, where an off-shell W^* radiates the final state. The charge factor of this diagram is unity.

The e_i are measured in units of e, so that $e_{q'} - e_q = 1$.

One can compute the $\Omega_j^{(0)}$ through the use of the projectors defined above, and once the three different contributions are known one can reconstruct the correct values for the helicity coefficients as:

$$\Omega_{W^{\pm}}^{(0)} = U_{qq'}\left(e_{q'}\,\Omega_1^{(0)} + e_q\,\Omega_2^{(0)} + \Omega_3^{(0)}\right) = U_{qq'}\left[e_{q'}\left(\Omega_1^{(0)} + \Omega_2^{(0)}\right) + \Omega_3^{(0)} - \Omega_2^{(0)}\right], \quad (3.1)$$

$$\Omega_{Z,\gamma^*}^{(0)} = e_q\left(\Omega_1^{(0)} + \Omega_2^{(0)}\right), \quad (3.2)$$

where U_{ij} are the CKM matrix elements. To simplify the expression above, we made use of the fact that the Z^0 boson does not couple to the photon, and that in this case there is no flavour change, i.e. $e_{q'} = e_q$.

At leading order, the d-dimensional expressions for the coefficients read:

$$\alpha_1^{(0)} = \frac{d-4}{4(d-3)}\left(2+\frac{v}{u}-\frac{1}{u}\right), \qquad \alpha_2^{(0)} = -\frac{d-4}{4(d-3)}\left(2+\frac{v}{u}-\frac{1}{u}\right)+1,$$
$$\alpha_3^{(0)} = -\frac{d-4}{4(d-3)}\left(2+\frac{v}{u}-\frac{1}{u}\right)+1-\frac{u}{1-v}. \tag{3.3}$$

$$\beta_1^{(0)} = \frac{d-4}{4(d-3)}\left(1-\frac{1}{u}\right)+1, \qquad \beta_2^{(0)} = -\frac{d-4}{4(d-3)}\left(1-\frac{1}{u}\right),$$
$$\beta_3^{(0)} = -\frac{d-4}{4(d-3)}\left(1-\frac{1}{u}\right)-\frac{u}{1-v}. \tag{3.4}$$

$$\gamma_1^{(0)} = -\frac{d-4}{4(d-3)}\left(1+\frac{v}{u}\right), \qquad \gamma_2^{(0)} = \frac{d-4}{4(d-3)}\left(1+\frac{v}{u}\right),$$
$$\gamma_3^{(0)} = \frac{d-4}{4(d-3)}\left(1+\frac{v}{u}\right). \tag{3.5}$$

Using (3.1) and (3.2) we find

$$\alpha_W^{(0)} = U_{qq'}\left(e_{q'}-\frac{u}{1-v}\right), \qquad \beta_W^{(0)} = U_{qq'}\left(e_{q'}-\frac{u}{1-v}\right), \qquad \gamma_W^{(0)} = 0, \tag{3.6}$$

$$\alpha_{Z,\gamma^*}^{(0)} = e_q, \qquad \beta_{Z,\gamma^*}^{(0)} = e_q, \qquad \gamma_{Z,\gamma^*}^{(0)} = 0. \tag{3.7}$$

At one-loop, the same classification of contributions applies: $I_1^{(1)}, I_2^{(1)}, I_3^{(1)}$. A further type of diagrams, with both the photon and the gauge boson which couple to a closed quark loop, is zero due to colour conservation. At two loops, besides $I_1^{(2)}, I_2^{(2)}, I_3^{(2)}$, three further classes of diagrams appear:

1. $I_4^{(2)}$ are the diagrams where both γ and V couple to the same fermion loop, as depicted for example in Figure 2, diagram (4).

   This contribution is denoted by $N_{F,V}$ and is proportional to the charge weighted sum of the quark flavours. In case of a γ^* exchange we find

   $$N_{F,\gamma} = \frac{\sum_{q'} e_{q'}^2}{e_q}\,. \tag{3.8}$$

   Considering Z-interactions, the same class of diagrams yields not only a contribution from the vector component of the Z, which for the right-handed quark amplitude is given by

   $$N_{F,Z} = \frac{\sum_{q'}\left(L^Z_{q'q'}+R^Z_{q'q'}\right)e_{q'}}{2R^Z_{qq}}\,, \tag{3.9}$$

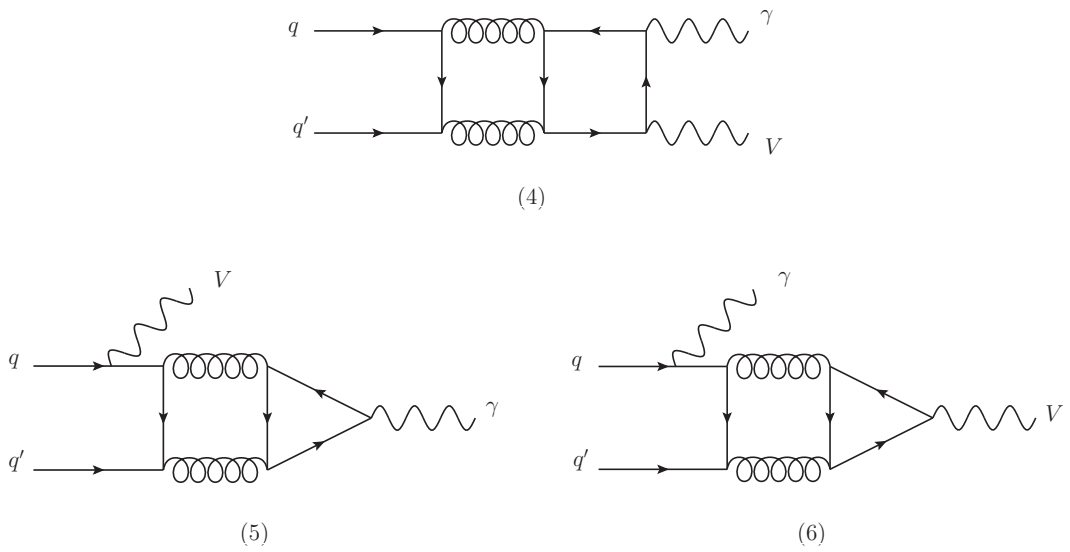

Figure 2: Examples of two-loop diagrams in the classes $I_4^{(2)}$, $I_5^{(2)}$ and $I_6^{(2)}$.

but also a contribution involving the axial couplings of the Z. This contribution vanishes identically for $Z^0\gamma$ production, already before summing over the quark flavours inside the loop. In the case of $W^\pm$ exchange charge conservation ensures that

$$N_{F,W^\pm} = 0. \tag{3.10}$$

2. $I_5^{(2)}$ are the diagrams where the photon couples alone to a fermion loop, while V couples to the fermion line, as depicted in Figure 2, diagram (5). This class of diagrams has to sum to zero due to Furry's theorem.

3. $I_6^{(2)}$ are finally the diagrams where V couples alone to a fermion loop, while γ couples to the fermion line, as depicted in Figure 2, diagram (6). These diagrams give both a vector and an axial contribution, where the vector contribution is again zero due to Furry's theorem, while the axial contribution is zero in the framework of massless QCD [21].

We explicitly evaluated the contributions from classes $I_5^{(2)}, I_6^{(2)}$, and their vanishing provides a check on our calculation.

The classes $I_j^{(2)},\ j = 1, 6$ exhaust all the possible two-loop QCD diagrams which can contribute to the production of a pair $V\,\gamma$, whatever is the identity of the vector boson V. When computing the helicity amplitudes, one can evaluate the contributions from these six classes of diagrams independently, without keeping track of the axial current contributions, thus considering the vector boson V as an off-shell purely vector particle. Once the $I_j^{(2)}$ are known, as for the tree-level case, one can reconstruct the proper amplitudes for $V = Z^0, W^\pm$ summing these six contributions up, multiplied by appropriate weights.

The calculation proceeds as follows. The 143 two-loop diagrams belonging to the classes $j = (1, 2, 4, 5, 6)$ are produced using QGRAF [26] while, on the other hand, we did not need to evaluate explicitly the diagrams in class $I_3^{(2)}$, since they only account for the QCD corrections of the quark form factor, which is known up to three loops in the literature [27, 28].

The tensor coefficients are then evaluated analytically diagram by diagram applying the projectors defined in [21]. As a result, one obtains the tensor coefficients in terms of thousands of planar and non-planar two-loop scalar integrals, which can be easily classified in two auxiliary topologies, one planar and the other non-planar [20]. Through the usual IBP identities [29] one can reduce independently all the integrals belonging to these two auxiliary topologies to a small set of master integrals. This reduction is performed using the Laporta algorithm [30], implemented in the Reduze code [31]. All the masters for such topologies are known [32] as series in the parameter $\epsilon = (4 - d)/2$, through a systematic approach based on the differential equation method [32, 33]. The masters are expressed as Laurent expansion in ϵ, with coefficients containing harmonic polylogarithms (HPLs, [34]) and two-dimensional harmonic polylogarithms (2dHPLs, [32]). Numerical implementations of these functions are available [35]. For all the intermediate algebraic manipulations we have made extensive use of FORM [36].

The two-loop unrenormalised helicity coefficients $\Omega^{(2),\mathrm{un}}$ can then be evaluated as linear combination of the tensor coefficients, and in particular they can be evaluated separately for every class of diagrams:

$$\Omega_j^{(2),\mathrm{un}}\,, \qquad \text{with } j = 1, 6\,. \tag{3.11}$$

As for the tree level case, it is trivial to reconstruct the amplitudes for the processes considered as linear combinations of these six amplitudes.

We start considering the case where $V = W^\pm$. The W boson couples only to left-handed fermions and charge conservation implies that $N_{F,W} = 0$. The amplitudes for $W^\pm\gamma$ production at two loops thus receive contributions only from three of the six classes of diagrams above, i.e.:

$$\begin{aligned}\Omega_{W^\pm}^{(2),\mathrm{un}} &= U_{qq'}\left(e_{q'}\,\Omega_1^{(2),\mathrm{un}} + e_q\,\Omega_2^{(2),\mathrm{un}} + \Omega_3^{(2),\mathrm{un}}\right)\\ &= U_{qq'}\left[e_{q'}\,\left(\Omega_1^{(2),\mathrm{un}} + \Omega_2^{(2),\mathrm{un}}\right) + \Omega_3^{(2),\mathrm{un}} - \Omega_2^{(2),\mathrm{un}}\right].\end{aligned} \tag{3.12}$$

As for the tree level, U_{ij} are the CKM matrix elements.

For the $V = Z^0, \gamma^*$ case, $I_3^{(n)} = 0$ at all orders, since the Z^0 and γ^* are electrically neutral, while $I_4^{(2)}$ is non-vanishing since charge conservation does not forbid such diagrams anymore.

$$\Omega_V^{(2),\mathrm{un}} = e_q\,\left(\Omega_1^{(2),\mathrm{un}} + \Omega_2^{(2),\mathrm{un}}\right) + N_{F,V}\,\Omega_4^{(2),\mathrm{un}}, \tag{3.13}$$

for $V = (Z^0, \gamma^*)$.

4. Two-loop helicity amplitudes

Renormalisation of ultraviolet divergences is performed in the $\overline{\rm MS}$ scheme by replacing the bare coupling α_0 with the renormalised coupling $\alpha_s \equiv \alpha_s(\mu^2)$, evaluated at the renormalisation scale μ^2. Since the tree amplitudes are of $\mathcal{O}(\alpha_s^0)$, we only need the one loop relation between the bare and renormalised couplings:

$$\alpha_0 \mu_0^{2\epsilon} S_\epsilon = \alpha_s \mu^{2\epsilon} \left[1 - \frac{\beta_0}{\epsilon} \left(\frac{\alpha_s}{2\pi} \right) + \mathcal{O}(\alpha_s^2) \right] , \tag{4.1}$$

where

$$S_\epsilon = (4\pi)^\epsilon e^{-\epsilon\gamma} \qquad \text{with Euler constant } \gamma = 0.5772\ldots$$

and μ_0^2 is the mass parameter introduced in dimensional regularisation to maintain a dimensionless coupling in the bare QCD Lagrangian density. β_0 is the first coefficient of the QCD β-function:

$$\beta_0 = \frac{11 C_A - 4 T_R N_F}{6}, \tag{4.2}$$

with the QCD colour factors

$$C_A = N, \qquad C_F = \frac{N^2-1}{2N}, \qquad T_R = \frac{1}{2} . \tag{4.3}$$

The renormalisation is performed at fixed scale $\mu^2 = q^2$. The renormalised helicity coefficients read:

$$\begin{aligned} \Omega^{(0)} &= \Omega^{(0),\rm un}, \\ \Omega^{(1)} &= S_\epsilon^{-1} \Omega^{(1),\rm un}, \\ \Omega^{(2)} &= S_\epsilon^{-2} \Omega^{(2),\rm un} - \frac{\beta_0}{\epsilon} S_\epsilon^{-1} \Omega^{(1),\rm un} . \end{aligned} \tag{4.4}$$

The full scale dependence of the coefficients can be recovered from the renormalisation group. It reads:

$$\begin{aligned} \Omega(\mu^2, \alpha_s(\mu^2)) = \sqrt{4\pi\alpha}\, \delta_{ij} \Bigg[& \Omega^{(0)} + \left(\frac{\alpha_s(\mu^2)}{2\pi} \right) \Omega^{(1)} \\ & + \left(\frac{\alpha_s(\mu^2)}{2\pi} \right)^2 \left(\Omega^{(2)} + \beta_0 \Omega^{(1)} \ln\left(\frac{\mu^2}{q^2} \right) \right) + \mathcal{O}(\alpha_s^3) \Bigg] , \end{aligned} \tag{4.5}$$

After performing ultraviolet renormalisation, the amplitudes still contain singularities, which are of infrared origin and will be analytically cancelled by those occurring in radiative processes of the same order. Catani [37] has shown how to organise the infrared pole structure of the one- and two-loop contributions renormalised in the $\overline{\rm MS}$-scheme in terms of the tree and renormalised one-loop amplitudes. The same procedure applies to the tensor coefficients. Their pole structure can be separated off as follows:

$\Omega^{(1)} = \boldsymbol{I}^{(1)}(\epsilon) \Omega^{(0)} + \Omega^{(1),\rm finite}$,

$$\Omega^{(2)} = \left(-\frac{1}{2}\boldsymbol{I}^{(1)}(\epsilon)\boldsymbol{I}^{(1)}(\epsilon) - \frac{\beta_0}{\epsilon}\boldsymbol{I}^{(1)}(\epsilon) + e^{-\epsilon\gamma}\frac{\Gamma(1-2\epsilon)}{\Gamma(1-\epsilon)}\left(\frac{\beta_0}{\epsilon}+K\right)\boldsymbol{I}^{(1)}(2\epsilon) + \boldsymbol{H}^{(2)}(\epsilon)\right)\Omega^{(0)} + \boldsymbol{I}^{(1)}(\epsilon)\Omega^{(1)} + \Omega^{(2),\text{finite}}, \tag{4.6}$$

where the constant K is

$$K = \left(\frac{67}{18} - \frac{\pi^2}{6}\right) C_A - \frac{10}{9} T_R N_F. \tag{4.7}$$

In our case, there is only a quark–antiquark pair present in the initial state, so that $\boldsymbol{I}^{(1)}(\epsilon)$ is given by,

$$\boldsymbol{I}^{(1)}(\epsilon) = -\frac{e^{\epsilon\gamma}}{2\Gamma(1-\epsilon)}\left[\frac{N^2-1}{2N}\left(\frac{2}{\epsilon^2}+\frac{3}{\epsilon}\right)\mathtt{S}_{12}\right], \tag{4.8}$$

where, since we have set $\mu^2 = s_{123}^2$:

$$\mathtt{S}_{12} = \left(-\frac{\mu^2}{s_{12}}\right)^{\epsilon} = (x)^{-\epsilon}\,(-1-i0)^{-\epsilon}\,. \tag{4.9}$$

Note that on expanding $\mathtt{S}_{12}$, imaginary parts are generated, the sign of which is fixed by the small imaginary part $+i0$ of s_{12}. The hard radiation constant is a scalar in colour space:

$$\boldsymbol{H}^{(2)}(\epsilon) = \frac{e^{\epsilon\gamma}}{4\,\epsilon\,\Gamma(1-\epsilon)} H^{(2)}. \tag{4.10}$$

with

$$H^{(2)} = 2H_q^{(2)} \tag{4.11}$$

where in the $\overline{\text{MS}}$ scheme

$$H_q^{(2)} = (N^2-1)\left[\left(\frac{7}{4}\zeta_3 + \frac{409}{864} - \frac{11\pi^2}{96}\right)N^2 + \left(\frac{3}{2}\zeta_3 + \frac{3}{32} - \frac{\pi^2}{8}\right)\frac{1}{N^2} + \left(\frac{\pi^2}{48} - \frac{25}{216}\right)\frac{N_F}{N}\right]. \tag{4.12}$$

For the infrared factorisation of the two-loop results, the renormalised next-to-leading order helicity amplitude coefficients are needed through to $\mathcal{O}(\epsilon^2)$. Their decomposition in colour structures is straightforward:

$$\Omega_j^{(1),\text{finite}}(u,v) = C_F\, a_\Omega^{(j)}(u,v)\,. \tag{4.13}$$

The expansion of the coefficients through to ϵ^2 yields HPLs and 2dHPLs up to weight 4. The explicit expressions are of considerable size, such that we only quote the ϵ^0-terms in the appendix. To this order, the coefficients had been derived previously [38, 39] in terms of logarithms and dilogarithms. The expressions through to $\mathcal{O}(\epsilon^2)$ in FORM format are appended to the arXiv submission of this article.

The finite two-loop remainder is obtained by subtracting the predicted infrared structure (expanded through to $\mathcal{O}(\epsilon^0)$) from the renormalised helicity coefficient. We further decompose the finite remainder according to the colour structures as follows:

$$\Omega_j^{(2),\text{finite}}(u,v) = (N^2-1)\left(A_\Omega^{(j)}(u,v) + \frac{1}{N^2}B_\Omega^{(j)}(u,v)\right) + C_F\,N_F C_\Omega^{(j)}(u,v) + C_F\,N_{F,V}D_\Omega^{(j)}(u,v)\,, \tag{4.14}$$

where the last term, as discussed above, is generated by graphs where the virtual gauge boson does not couple directly to the final-state quarks, and is different from zero only for the $V = Z, \gamma^*$ case.

The helicity coefficients contain HPLs and 2dHPLs up to weight 4. The size of each helicity coefficient is comparable to the size of the helicity-averaged tree times two-loop matrix element for $3j$ production quoted in [20], and we decided not to include them here explicitly. The complete set of coefficients in FORM format is attached to the arXiv submission of this article.

5. Checks on the result

Several non-trivial checks were applied to validate our results:

1. All seven tensor coefficients in (2.10) were computed. We validated that they fulfil the following relations, which follow from the symmetry properties of the tensor under an interchange $p_1 \leftrightarrow p_2$:

$$\begin{aligned} A_{21}(s_{13},s_{23},s_{123}) &= -A_{12}(s_{23},s_{13},s_{123}),\\ A_{22}(s_{13},s_{23},s_{123}) &= -A_{11}(s_{23},s_{13},s_{123}),\\ A_{23}(s_{13},s_{23},s_{123}) &= -A_{13}(s_{23},s_{13},s_{123}),\\ B(s_{13},s_{23},s_{123}) &= B(s_{23},s_{13},s_{123}). \end{aligned} \tag{5.1}$$

2. We computed explicitly the helicity coefficients for all the diagrams in classes $I_5^{(2)}$ and $I_6^{(2)}$, which should yield a vanishing contribution due to Furry's theorem. Each diagram gives a non-vanishing contribution, a full cancellation is obtained only in the sum of all diagrams.

3. The IR singularity structure of our result agrees with the prediction of the Catani formula [37].

4. We compared the helicity coefficients $\Omega_Z^{(2)}$ for $q\bar{q} \to Z\gamma$, with those for $\gamma^* \to q\bar{q}g$ [21]. As explained in Appendix C, the unrenormalised two-loop Ω_{3j} coefficients can be decomposed according to their colour structure as:

$$\Omega_{3j}^{(2,\text{un})}(u,v) = N^2 A_\Omega^{(3j,\text{un})}(u,v) + B_\Omega^{(3j,\text{un})}(u,v) + \frac{1}{N^2}C_\Omega^{(3j,\text{un})}(u,v) + N N_F D_\Omega^{(3j,\text{un})}(u,v) + \frac{N_F}{N}E_\Omega^{(3j,\text{un})}(u,v) + N_F^2 F_\Omega^{(3j,\text{un})}(u,v)$$

$$+ N_{F,V} \left(\frac{4}{N} - N \right) G_\Omega^{(3j,\mathrm{un})}(u,v) \,. \tag{5.2}$$

We checked that in the decay kinematical configuration $Z \to q\,\bar{q}\,\gamma$, prior to UV renormalisation and IR subtraction, the following identities are fulfilled

$$\begin{aligned} B_\Omega^{(Z,\mathrm{un})}(y,z) &= - \; C_\Omega^{(3j,\mathrm{un})}(y,z) \,, \\ C_\Omega^{(Z,\mathrm{un})}(y,z) &= - \, 2\, E_\Omega^{(3j,\mathrm{un})}(y,z) \,, \\ D_\Omega^{(Z,\mathrm{un})}(y,z) &= - \, 4\, G_\Omega^{(3j,\mathrm{un})}(y,z) \,, \end{aligned} \tag{5.3}$$

which follow from the structure of the underlying two-loop diagrams. UV renormalisation and IR subtraction of the $Z \to q\bar{q}\gamma$ and $Z \to q\bar{q}g$ amplitudes differ. However, two of the above relations are unaffected by renormalisation and retain the same IR structure, such that we obtain:

$$\begin{aligned} B_\Omega^{(Z,\mathrm{finite})}(u,v) &= - \; C_\Omega^{(3j,\mathrm{finite})}(u,v) \,, \\ D_\Omega^{(Z,\mathrm{finite})}(u,v) &= - \, 4\, G_\Omega^{(3j,\mathrm{finite})}(u,v) \,, \end{aligned} \tag{5.4}$$

which also remain true after analytic continuation.

6. Conclusions and Outlook

In this paper we derived the two-loop corrections to the helicity amplitudes for the processes $q\bar{q} \to W^\pm\gamma$ and $q\bar{q} \to Z^0\gamma$. Our calculation was performed in dimensional regularisation by applying d-dimensional projection operators to the most general tensor structure of the amplitude. Our results are expressed in terms of dimensionless helicity coefficients, which multiply the basic tree-level amplitudes, expressed in four-dimensional spinors. By applying Catani's infrared factorisation formula, we extract the finite parts of the helicity coefficients, which are independent on the precise scheme used to define the helicity amplitudes. We provide compact analytic expressions for the two-loop helicity coefficients in terms of HPLs and 2dHPLs.

These amplitudes are relevant to the NNLO corrections to $V\gamma$ production at hadron colliders. This process provides a direct access to the photonic couplings of the weak gauge bosons and is a crucial test of the structure of the electroweak theory at high energies. With the amplitudes derived here, in combination with the amplitudes relevant to $V\gamma j$ production at NLO [9], all ingredients to this NNLO calculation are now available. Since the leading order contribution to this process does not contain any QCD partons in the final state, the well-established q_T subtraction method [12] could be used for this calculation.

Acknowledgements

This research was supported in part by the Swiss National Science Foundation (SNF) under contract PDFMP2-135101 and by the European Commission through the "LHCPhenoNet" Initial Training Network PITN-GA-2010-264564.

A. One-loop helicity amplitudes

We list here the ϵ^0-terms of the one-loop helicity coefficients for the groups of diagrams defined above:

$$
\begin{aligned}
a_\alpha^{(1)} &= \zeta_2 + G(-v,u)i\,\pi\, - G(-v,u)H(0,v) + G(-v,0,u) + G(0,u)H(0,v) + H(0,v)i\,\pi \\
&\quad - H(0,0,v) + H(1,0,v) + \mathcal{O}(\epsilon)\,, \\
a_\alpha^{(2)} &= \frac{(1-v)^2}{u^2}\left[G(1-v,u)H(0,v) + G(1,1-v,u) + G(1,u)i\,\pi\, - G(1,u)H(0,v)\right. \\
&\quad \left. - G(1,u)H(1,v)\right] + \frac{(1-u-v)(2-2v-u+3uv-u^2)}{2u(1-u)^2}\left[i\,\pi\, + G(1-v,u) - H(1,v)\right] \\
&\quad + \frac{v(2-2v-2u+3uv)}{2u(1-u)^2}\,H(0,v) + \frac{(7u-7-v)}{2(1-u)} + \mathcal{O}(\epsilon)\,, \\
a_\alpha^{(3)} &= -\frac{4(1-u-v)}{(1-v)} + \mathcal{O}(\epsilon)\,,
\end{aligned}
\tag{A.1}
$$

$$
\begin{aligned}
a_\beta^{(1)} &= \zeta_2 + G(-v,u)i\,\pi\, - G(-v,u)H(0,v) + G(-v,0,u) + G(0,u)H(0,v) + H(0,v)i\,\pi \\
&\quad - H(0,0,v) + H(1,0,v) + \frac{v(-3+3v+u)}{2(1-v)^2}\,H(0,v) + \frac{(-9+9v+u)}{2(1-v)} + \mathcal{O}(\epsilon) \\
a_\beta^{(2)} &= \frac{(1-v+uv)}{u^2}\left[G(1-v,u)H(0,v) + G(1,1-v,u) + G(1,u)i\,\pi\, - G(1,u)H(0,v)\right. \\
&\quad \left. - G(1,u)H(1,v)\right] + \frac{(2-2v-u+3uv-u^2)}{2u(1-u)}\left[i\,\pi\, + G(1-v,u) - H(1,v)\right] \\
&\quad + \frac{v(2-4v+2v^2+3uv-3uv^2-2u^2+3u^2v-u^3)}{2u(1-u)(1-v)^2}\,H(0,v) + \frac{(1-v+u)}{2(1-v)} + \mathcal{O}(\epsilon)\,, \\
a_\beta^{(3)} &= \frac{4u}{(1-v)} + \mathcal{O}(\epsilon)\,,
\end{aligned}
\tag{A.2}
$$

$$
\begin{aligned}
a_\gamma^{(1)} &= \frac{v(1-u-v)}{2(1-v)^2}\,H(0,v) + \frac{(1-u-v)}{2(1-v)} + \mathcal{O}(\epsilon)\,, \\
a_\gamma^{(2)} &= \frac{v(1-u-v)}{u^2}\left[G(1-v,u)H(0,v) + G(1,1-v,u) + G(1,u)i\,\pi\, - G(1,u)H(0,v)\right. \\
&\quad \left. - G(1,u)H(1,v)\right] + \frac{v(1-u-v)(2-3u)}{2u(1-u)^2}\left[i\,\pi\, + G(1-v,u) - H(1,v)\right] \\
&\quad + \frac{(1-u-v)(v-u)}{2(1-u)(1-v)} + \frac{v(1-u-v)(2v-2v^2-2uv+3uv^2-2u^2v+u^3)}{2u(1-u)^2(1-v)^2}\,H(0,v) + \mathcal{O}(\epsilon)\,, \\
a_\gamma^{(3)} &= \mathcal{O}(\epsilon)\,.
\end{aligned}
\tag{A.3}
$$

It should also be noted that these finite pieces of the one-loop coefficients can equally be written in terms of ordinary logarithms and dilogarithms, see [38, 39]. The reason to express them in terms of HPLs and 2dHPLs here is their usage in the infrared counter-term

of the two-loop coefficients, which cannot be fully expressed in terms of logarithmic and polylogarithmic functions.

B. Two-loop leading colour amplitudes

The analytical expressions for the finite remainders of the two-loop amplitudes, as defined in (4.14), are of considerable size. For illustration, we only quote the leading colour contributions here.

$$
\begin{aligned}
A_\alpha^{(1)} = \frac{1}{4}\Big[& - G(-v,1-v,-v,u)\,i\,\pi + G(-v,1-v,-v,u)\,H(0,v) - G(-v,1-v,-v,0,u) \\
& - G(-v,1-v,u)\,\zeta_2 - G(-v,1-v,u)\,H(0,v)\,i\,\pi + G(-v,1-v,u)\,H(0,0,v) \\
& - G(-v,1-v,u)\,H(1,0,v) - G(-v,1-v,0,u)\,H(0,v) - 2\,G(-v,-v,-v,u)\,i\,\pi \\
& + 2\,G(-v,-v,-v,u)\,H(0,v) - 2\,G(-v,-v,-v,0,u) - 4\,G(-v,-v,u)\,\zeta_2 \\
& - 2\,G(-v,-v,u)\,H(0,v)\,i\,\pi + 2\,G(-v,-v,u)\,H(0,0,v) + 2\,G(-v,-v,0,u)\,i\,\pi \\
& - 2\,G(-v,-v,0,u)\,H(0,v) + 2\,G(-v,-v,0,0,u) - 2\,G(-v,u)\,\zeta_3 \\
& - G(-v,u)\,i\,\pi\,\zeta_2 - 3\,G(-v,u)\,H(0,0,v)\,i\,\pi + 3\,G(-v,u)\,H(0,0,0,v) \\
& - G(-v,u)\,H(0,1,0,v) + G(-v,u)\,H(1,v)\,\zeta_2 + G(-v,u)\,H(1,0,v)\,i\,\pi \\
& - G(-v,u)\,H(1,0,0,v) + G(-v,u)\,H(1,1,0,v) + 3\,G(-v,0,-v,u)\,i\,\pi \\
& - 3\,G(-v,0,-v,u)\,H(0,v) + 3\,G(-v,0,-v,0,u) - G(-v,0,u)\,\zeta_2 \\
& + 2\,G(-v,0,u)\,H(0,v)\,i\,\pi - 3\,G(-v,0,u)\,H(0,0,v) + G(-v,0,u)\,H(1,0,v) \\
& + 2\,G(-v,0,0,u)\,H(0,v) + 2\,G(0,1-v,-v,u)\,i\,\pi - 2\,G(0,1-v,-v,u)\,H(0,v) \\
& + 2\,G(0,1-v,-v,0,u) + 2\,G(0,1-v,u)\,\zeta_2 + 2\,G(0,1-v,u)\,H(0,v)\,i\,\pi \\
& - 2\,G(0,1-v,u)\,H(0,0,v) + 2\,G(0,1-v,u)\,H(1,0,v) + 2\,G(0,1-v,0,u)\,H(0,v) \\
& + 2\,G(0,-v,-v,u)\,i\,\pi - 2\,G(0,-v,-v,u)\,H(0,v) + 2\,G(0,-v,-v,0,u) \\
& - 2\,G(0,-v,u)\,\zeta_2 + G(0,-v,u)\,H(0,v)\,i\,\pi - 2\,G(0,-v,u)\,H(0,0,v) \\
& + G(0,-v,0,u)\,H(0,v) - G(0,u)\,H(0,v)\,\zeta_2 + 2\,G(0,u)\,H(0,0,v)\,i\,\pi \\
& - 3\,G(0,u)\,H(0,0,0,v) + G(0,u)\,H(0,1,0,v) + 2\,G(0,u)\,H(1,0,0,v) - 2\,G(0,0,-v,u)\,i\,\pi \\
& + 2\,G(0,0,-v,u)\,H(0,v) - 2\,G(0,0,-v,0,u) + 2\,G(0,0,u)\,H(0,0,v) - 2\,H(0,v)\,\zeta_3 \\
& - H(0,v)\,i\,\pi\,\zeta_2 - 3\,H(0,0,0,v)\,i\,\pi + 3\,H(0,0,0,0,v) - H(0,0,1,0,v) + H(0,1,v)\,\zeta_2 \\
& + H(0,1,0,v)\,i\,\pi - H(0,1,0,0,v) + H(0,1,1,0,v) + 2\,H(1,v)\,\zeta_3 \\
& + 2\,H(1,0,v)\,\zeta_2 + 2\,H(1,0,0,v)\,i\,\pi - 2\,H(1,0,0,0,v) + 2\,H(1,0,1,0,v) + 2\,H(1,1,0,0,v)\Big] \\
& - \frac{5}{16}\,\zeta_4 + \frac{11}{12}\Big[- G(-v,-v,u)\,i\,\pi + G(-v,-v,u)\,H(0,v) - G(-v,-v,0,u) \\
& - G(-v,u)\,H(0,0,v) + G(-v,0,u)\,H(0,v) - G(-v,0,0,u) - G(0,0,u)\,H(0,v)\Big] \\
& - \frac{5}{4}\Big[G(-v,u)\,H(0,v)\,\zeta_2 + H(0,0,v)\,\zeta_2\Big] - \frac{11}{6}\,G(-v,u)\,\zeta_2 \\
& + \frac{v}{16\,(u+v)^2}\Big(1 - 3\,v - 3\,u\Big)\,H(0,v) \\
& + \frac{v}{8\,u\,(1-u)^3}\Big(2 - 2\,v - 4\,u + 5\,u\,v + 4\,u^2 - 5\,u^2\,v - 2\,u^3\Big)\Big[- G(0,-v,u)\,i\,\pi \\
& + G(0,-v,u)\,H(0,v) - G(0,-v,0,u)\Big]
\end{aligned}
$$

$$
+\frac{(1-u-v)}{8\,u\,(1-u)^3}\left(2-2\,v-3\,u+5\,u\,v-5\,u^2\,v+u^3\right)\Big[-2\,i\,\pi\,\zeta_2-H(1,0,v)\,i\,\pi\Big]
$$
$$
+\frac{(1-u-v)}{4\,u^2}\left(1-v+u\right)\Big[+G(1-v,1-v,-v,u)\,i\,\pi-G(1-v,1-v,-v,u)\,H(0,v)
$$
$$
+G(1-v,1-v,-v,0,u)+G(1-v,1-v,u)\,\zeta_2+G(1-v,1-v,u)\,H(0,v)\,i\,\pi
$$
$$
-G(1-v,1-v,u)\,H(0,0,v)+G(1-v,1-v,u)\,H(1,0,v)+G(1-v,1-v,0,u)\,H(0,v)
$$
$$
+G(1-v,u)\,\zeta_3+G(1-v,u)\,H(0,v)\,\zeta_2+G(1-v,u)\,H(0,0,v)\,i\,\pi
$$
$$
-G(1-v,u)\,H(0,0,0,v)+G(1-v,u)\,H(0,1,0,v)+G(1-v,u)\,H(1,0,0,v)
$$
$$
-G(1-v,0,-v,u)\,i\,\pi+G(1-v,0,-v,u)\,H(0,v)-G(1-v,0,-v,0,u)
$$
$$
+G(1-v,0,u)\,H(0,0,v)+G(1,1-v,-v,u)\,i\,\pi-G(1,1-v,-v,u)\,H(0,v)
$$
$$
+G(1,1-v,-v,0,u)+G(1,1-v,u)\,\zeta_2+G(1,1-v,u)\,H(0,v)\,i\,\pi
$$
$$
-G(1,1-v,u)\,H(0,0,v)+G(1,1-v,u)\,H(1,0,v)+G(1,1-v,0,u)\,H(0,v)
$$
$$
+G(1,u)\,\zeta_3-2\,G(1,u)\,i\,\pi\,\zeta_2-G(1,u)\,H(0,v)\,\zeta_2-G(1,u)\,H(0,0,v)\,i\,\pi
$$
$$
+G(1,u)\,H(0,0,0,v)-G(1,u)\,H(0,1,0,v)-G(1,u)\,H(1,v)\,\zeta_2-G(1,u)\,H(1,0,v)\,i\,\pi
$$
$$
+G(1,u)\,H(1,0,0,v)-G(1,u)\,H(1,1,0,v)+G(1,0,-v,u)\,i\,\pi-G(1,0,-v,u)\,H(0,v)
$$
$$
+G(1,0,-v,0,u)-2\,G(1,0,u)\,\zeta_2-G(1,0,u)\,H(0,0,v)-G(1,0,u)\,H(1,0,v)\Big]
$$
$$
+\frac{1}{16\,(1-u)\,(u+v)^2}\left(-v-v^2+2\,v^3-4\,u\,v+5\,u\,v^2-4\,u^2+7\,u^2\,v+4\,u^3\right)\Big[i\,\pi+G(0,u)\Big]
$$
$$
+\frac{1}{144\,(1-u)^2\,(1-u-v)}\Big(313-331\,v+18\,v^2-975\,u+716\,u\,v-54\,u\,v^2+1011\,u^2
$$
$$
-385\,u^2\,v-349\,u^3\Big)\Big[G(0,u)\,H(0,v)+H(0,v)\,i\,\pi\Big]
$$
$$
+\frac{1}{16\,u\,(u+v)}\left(-8\,v+8\,v^2-9\,u+25\,u\,v+17\,u^2\right)
$$
$$
+\frac{1}{144\,u\,(1-u)^2\,(1-u-v)}\Big(36-108\,v+108\,v^2-36\,v^3+169\,u+29\,u\,v-270\,u\,v^2
$$
$$
+72\,u\,v^3-759\,u^2+320\,u^2\,v+126\,u^2\,v^2+867\,u^3-241\,u^3\,v-313\,u^4\Big)\,H(1,0,v)
$$
$$
+\frac{1}{144\,u\,(1-u)^2\,(1-u-v)}\Big(72-216\,v+216\,v^2-72\,v^3+25\,u+389\,u\,v-558\,u\,v^2
$$
$$
+144\,u\,v^3-543\,u^2-76\,u^2\,v+306\,u^2\,v^2+723\,u^3-97\,u^3\,v-277\,u^4\Big)\,\zeta_2
$$
$$
+\frac{1}{144\,u\,(1-u)^2\,(1-u-v)}\left(-36\,v+72\,v^2-36\,v^3-313\,u+475\,u\,v-234\,u\,v^2\right.
$$
$$
\left.+72\,u\,v^3+975\,u^2-896\,u^2\,v+198\,u^2\,v^2-1011\,u^3+457\,u^3\,v+349\,u^4\right)\Big[-G(-v,u)\,i\,\pi
$$
$$
+G(-v,u)\,H(0,v)-G(-v,0,u)+H(0,0,v)\Big]
$$
$$
+\frac{1}{8\,u\,(1-u)^3}\Big(4-6\,v+2\,v^2-10\,u+16\,u\,v-5\,u\,v^2+6\,u^2-16\,u^2\,v+5\,u^2\,v^2
$$
$$
+2\,u^3+6\,u^3\,v-2\,u^4\Big)\Big[G(1-v,-v,u)\,i\,\pi-G(1-v,-v,u)\,H(0,v)+G(1-v,-v,0,u)
$$
$$
+G(1-v,u)\,\zeta_2+G(1-v,u)\,H(0,v)\,i\,\pi-G(1-v,u)\,H(0,0,v)+G(1-v,u)\,H(1,0,v)
$$
$$
+G(1-v,0,u)\,H(0,v)\Big]
$$
$$
-\frac{1}{12\,u\,(1-u)^3}\Big(6-12\,v+6\,v^2-4\,u+30\,u\,v-15\,u\,v^2-24\,u^2-30\,u^2\,v+15\,u^2\,v^2
$$

$$
\begin{aligned}
&+ 36\,u^3 + 12\,u^3\,v - 14\,u^4\Big)\,G(0,u)\,\zeta_2 \\
&+ \frac{1}{24\,u\,(1-u)^3}\Big(6 - 12\,v + 6\,v^2 + 7\,u + 30\,u\,v - 15\,u\,v^2 - 57\,u^2 - 30\,u^2\,v + 15\,u^2\,v^2 \\
&+ 69\,u^3 + 12\,u^3\,v - 25\,u^4\Big)\Big[- G(0,u)\,H(1,0,v) - H(1,v)\,\zeta_2 - H(1,1,0,v)\Big] \\
&+ \frac{1}{24\,u\,(1-u)^3}\Big(12 - 18\,v + 6\,v^2 - 8\,u + 48\,u\,v - 15\,u\,v^2 - 48\,u^2 - 48\,u^2\,v + 15\,u^2\,v^2 \\
&+ 72\,u^3 + 18\,u^3\,v - 28\,u^4\Big)\,\zeta_3 \\
&+ \frac{1}{24\,u\,(1-u)^3}\Big(12 - 18\,v + 6\,v^2 + 14\,u + 48\,u\,v - 15\,u\,v^2 - 114\,u^2 - 48\,u^2\,v + 15\,u^2\,v^2 \\
&+ 138\,u^3 + 18\,u^3\,v - 50\,u^4,\Big)\,H(1,0,0,v) \\
&+ \frac{1}{24\,u\,(1-u)^3}\Big(- 6\,v + 6\,v^2 - 44\,u + 12\,u\,v - 15\,u\,v^2 + 132\,u^2 - 12\,u^2\,v + 15\,u^2\,v^2 \\
&- 132\,u^3 + 6\,u^3\,v + 44\,u^4\Big)\Big[- G(0,u)\,H(0,0,v) + H(0,0,0,v)\Big] \\
&+ \frac{1}{24\,u\,(1-u)^3}\Big(- 6\,v + 6\,v^2 - 22\,u + 12\,u\,v - 15\,u\,v^2 + 66\,u^2 - 12\,u^2\,v + 15\,u^2\,v^2 \\
&- 66\,u^3 + 6\,u^3\,v + 22\,u^4\Big)\Big[- H(0,0,v)\,i\,\pi - H(0,1,0,v)\Big] \\
&+ \frac{1}{24\,u\,(1-u)^3}\Big(6\,v - 6\,v^2 - 22\,u - 12\,u\,v + 15\,u\,v^2 + 66\,u^2 + 12\,u^2\,v - 15\,u^2\,v^2 \\
&- 66\,u^3 - 6\,u^3\,v + 22\,u^4\Big)\,H(0,v)\,\zeta_2\,,
\end{aligned}
$$

$$
\begin{aligned}
A_\alpha^{(2)} = &- \frac{11}{16}\,H(0,v)\,\zeta_2 + \frac{49}{32}\,\zeta_4 + \frac{7}{4}\Big[i\,\pi\,\zeta_3 + H(0,v)\,\zeta_3\Big] \\
&+ \frac{(1-v)^2}{4\,u^2}\Bigg[\frac{13}{6}\,G(1,u)\,H(0,v)\,i\,\pi - \frac{35}{6}\,G(1,u)\,H(0,1,v) + \frac{22}{3}\,G(1-v,u)\,H(0,0,v) \\
&- \frac{22}{3}\,G(1,u)\,H(0,0,v) + 2\,G(1-v,1-v,u)\,\zeta_2 + 2\,G(1-v,1-v,u)\,H(0,v)\,i\,\pi \\
&- 2\,G(1-v,1-v,u)\,H(0,1,v) - 2\,G(1-v,1-v,1,1-v,u) - 2\,G(1-v,1-v,1,u)\,i\,\pi \\
&+ 2\,G(1-v,1-v,1,u)\,H(0,v) + 2\,G(1-v,1-v,1,u)\,H(1,v) + 2\,G(1-v,0,1-v,u)\,H(0,v) \\
&+ 2\,G(1-v,0,1,1-v,u) + 2\,G(1-v,0,1,u)\,i\,\pi - 2\,G(1-v,0,1,u)\,H(0,v) \\
&- 2\,G(1-v,0,1,u)\,H(1,v) + G(1-v,1,1-v,u)\,H(0,v) - 4\,G(1-v,1,u)\,\zeta_2 \\
&- G(1-v,1,u)\,H(0,v)\,i\,\pi + G(1-v,1,u)\,H(0,1,v) - G(1-v,1,u)\,H(1,0,v) \\
&+ 2\,G(1-v,1,1,1-v,u) + 2\,G(1-v,1,1,u)\,i\,\pi - 2\,G(1-v,1,1,u)\,H(0,v) \\
&- 2\,G(1-v,1,1,u)\,H(1,v) + 2\,G(1,1-v,1-v,u)\,H(0,v) - 4\,G(1,1-v,u)\,\zeta_2 \\
&- G(1,1-v,u)\,H(0,v)\,i\,\pi + G(1,1-v,u)\,H(0,1,v) - G(1,1-v,u)\,H(1,0,v) \\
&+ 3\,G(1,1-v,1,1-v,u) + 3\,G(1,1-v,1,u)\,i\,\pi - 3\,G(1,1-v,1,u)\,H(0,v) \\
&- 3\,G(1,1-v,1,u)\,H(1,v) - 3\,G(1,u)\,\zeta_3 - G(1,u)\,i\,\pi\,\zeta_2 + 4\,G(1,u)\,H(1,v)\,\zeta_2 \\
&+ G(1,u)\,H(1,0,v)\,i\,\pi - G(1,u)\,H(1,0,1,v) + G(1,u)\,H(1,1,0,v) \\
&- G(1,0,1-v,u)\,H(0,v) - G(1,0,1,1-v,u) - G(1,0,1,u)\,i\,\pi + G(1,0,1,u)\,H(0,v) \\
&+ G(1,0,1,u)\,H(1,v) + 2\,G(1,1,1-v,1-v,u) + 2\,G(1,1,1-v,u)\,i\,\pi \\
&- 2\,G(1,1,1-v,u)\,H(0,v) - 2\,G(1,1,1-v,u)\,H(1,v) - 2\,G(1,1,u)\,\zeta_2
\end{aligned}
$$

$$
\begin{aligned}
&- 2\,G(1,1,u)\,H(1,v)\,i\,\pi + 2\,G(1,1,u)\,H(1,0,v) + 2\,G(1,1,u)\,H(1,1,v) \\
&- 2\,G(1,1,1,1-v,u) - 2\,G(1,1,1,u)\,i\,\pi + 2\,G(1,1,1,u)\,H(0,v) + 2\,G(1,1,1,u)\,H(1,v)\Big] \\
&+ \frac{11\,v}{12\,u\,(1-u)^2}\Big(2 - 2\,v - 2\,u + 3\,u\,v\Big)\,H(0,0,v) \\
&+ \frac{(1-u-v)}{8\,u\,(1-u)^2}\Big(2 - 2\,v - u + 3\,u\,v - u^2\Big)\Big[- G(1-v,u)\,H(1,0,v) + H(1,0,v)\,i\,\pi \\
&- H(1,0,1,v) + H(1,1,0,v)\Big] \\
&+ \frac{(1-u-v)}{16\,u\,(1-u)^2}\Big(6 - 6\,v - 3\,u + 5\,u\,v - 3\,u^2\Big)\Big[G(1-v,u)\,i\,\pi - H(1,v)\,i\,\pi\Big] \\
&- \frac{(1-u-v)}{24\,u\,(1-u)^2}\Big(22 - 22\,v - 11\,u + 39\,u\,v - 11\,u^2\Big)\,H(1,0,v) \\
&+ \frac{(1-u-v)}{48\,u\,(1-u)^2}\Big(26 - 26\,v - 13\,u + 51\,u\,v - 13\,u^2\Big)\Big[- G(1-v,1-v,u) \\
&+ G(1-v,u)\,H(1,v) - H(1,1,v)\Big] \\
&+ \frac{(1-u-v)}{288\,u\,(1-u)^2}\Big(- 554 + 288\,\zeta_2 + 554\,v - 288\,v\,\zeta_2 + 433\,u - 144\,u\,\zeta_2 - 909\,u\,v \\
&+ 432\,u\,v\,\zeta_2 + 121\,u^2 - 144\,u^2\,\zeta_2\Big)\,H(1,v) \\
&+ \frac{(1-u-v)}{288\,u\,(1-u)^2}\Big(554 - 554\,v - 433\,u + 909\,u\,v - 121\,u^2\Big)\,G(1-v,u) \\
&+ \frac{(1-u-v)}{8\,u^2\,(1-u)^2}\Big(3 - 3\,v - u + 2\,u\,v - u^2 + 3\,u^2\,v - u^3\Big)\Big[G(1,1-v,u)\,i\,\pi - G(1,u)\,H(1,v)\,i\,\pi\Big] \\
&+ \frac{1}{10368\,u\,(1-u)}\Big(5184 - 5184\,v - 87239\,u - 4788\,u\,v + 82055\,u^2\Big) \\
&+ \frac{1}{8\,u\,(1-u)^2}\Big(2 - 8\,v + 6\,v^2 - 3\,u + 10\,u\,v - 9\,u\,v^2 - 2\,u^2\,v + u^3\Big)\Big[G(1-v,1,1-v,u) \\
&+ G(1-v,1,u)\,i\,\pi - G(1-v,1,u)\,H(0,v) - G(1-v,1,u)\,H(1,v)\Big] \\
&+ \frac{1}{8\,u\,(1-u)^2}\Big(2 - 2\,v^2 - 3\,u + 2\,u\,v + 3\,u\,v^2 - 2\,u^2\,v + u^3\Big)\Big[G(0,1-v,u)\,H(0,v) \\
&+ G(0,1,1-v,u) + G(0,1,u)\,i\,\pi - G(0,1,u)\,H(0,v) - G(0,1,u)\,H(1,v)\Big] \\
&- \frac{1}{48\,u\,(1-u)^2}\Big(44 - 114\,v + 70\,v^2 - 66\,u + 158\,u\,v - 105\,u\,v^2 - 44\,u^2\,v + 22\,u^3\Big)\,H(0,1,v) \\
&+ \frac{1}{48\,u\,(1-u)^2}\Big(44 - 70\,v + 26\,v^2 - 66\,u + 114\,u\,v - 39\,u\,v^2 - 44\,u^2\,v + 22\,u^3\Big)\,H(0,v)\,i\,\pi \\
&- \frac{1}{144\,u\,(1-u)^2}\Big(480\,\zeta_2 + 108\,\zeta_3 - 882\,v\,\zeta_2 - 216\,v\,\zeta_3 + 402\,v^2\,\zeta_2 + 108\,v^2\,\zeta_3 - 660\,u\,\zeta_2 \\
&- 551\,u\,\zeta_3 + 1326\,u\,v\,\zeta_2 + 324\,u\,v\,\zeta_3 - 567\,u\,v^2\,\zeta_2 - 162\,u\,v^2\,\zeta_3 - 120\,u^2\,\zeta_2 + 778\,u^2\,\zeta_3 \\
&- 444\,u^2\,v\,\zeta_2 - 108\,u^2\,v\,\zeta_3 + 300\,u^3\,\zeta_2 - 335\,u^3\,\zeta_3\Big) \\
&- \frac{1}{864\,u\,(1-u)^2}\Big(- 1662 + 216\,\zeta_2 + 3324\,v - 432\,v\,\zeta_2 - 1662\,v^2 + 216\,v^2\,\zeta_2 + 5324\,u \\
&+ 270\,u\,\zeta_2 - 5292\,u\,v + 648\,u\,v\,\zeta_2 + 2727\,u\,v^2 - 324\,u\,v^2\,\zeta_2 - 5662\,u^2 - 1188\,u^2\,\zeta_2 + 1968\,u^2\,v \\
&- 216\,u^2\,v\,\zeta_2 + 2000\,u^3 + 702\,u^3\,\zeta_2\Big)\,i\,\pi
\end{aligned}
$$

$$
\begin{aligned}
&- \frac{1}{864\,u\,(1-u)^2}\Big(- 1662\,v + 1662\,v^2 + 2363\,u + 2526\,u\,v - 2727\,u\,v^2 - 4726\,u^2 - 864\,u^2\,v \\
&+ 2363\,u^3\Big)\,H(0,v) \\
&+ \frac{1}{8\,u^2\,(1-u)^2}\Big(3 - 6\,v + 3\,v^2 - 6\,u + 14\,u\,v - 8\,u\,v^2 + 3\,u^2 - 8\,u^2\,v + 6\,u^2\,v^2\Big) \\
&\times G(1-v,u)\,H(0,v)\,i\,\pi \\
&+ \frac{1}{24\,u^2\,(1-u)^2}\Big(13 - 26\,v + 13\,v^2 - 32\,u + 70\,u\,v - 38\,u\,v^2 + 22\,u^2 - 50\,u^2\,v + 31\,u^2\,v^2 \\
&+ 6\,u^3\,v - 3\,u^4\Big)\Big[- G(1-v,1-v,u)\,H(0,v) - G(1,1-v,1-v,u) + G(1,1-v,u)\,H(1,v) \\
&- G(1,u)\,H(1,1,v)\Big] \\
&+ \frac{1}{24\,u^2\,(1-u)^2}\Big(13 - 26\,v + 13\,v^2 - 26\,u + 46\,u\,v - 20\,u\,v^2 + 13\,u^2 - 20\,u^2\,v + 4\,u^2\,v^2\Big) \\
&\times G(1-v,u)\,H(0,1,v) \\
&+ \frac{1}{24\,u^2\,(1-u)^2}\Big(13 - 26\,v + 13\,v^2 - 20\,u + 34\,u\,v - 14\,u\,v^2 + 4\,u^2 - 2\,u^2\,v - 5\,u^2\,v^2 - 6\,u^3\,v \\
&+ 3\,u^4\Big)\Big[- G(1,1,1-v,u) - G(1,1,u)\,i\,\pi + G(1,1,u)\,H(0,v) + G(1,1,u)\,H(1,v)\Big] \\
&- \frac{1}{24\,u^2\,(1-u)^2}\Big(13 - 26\,v + 13\,v^2 - 8\,u + 10\,u\,v - 2\,u\,v^2 - 14\,u^2 + 34\,u^2\,v - 23\,u^2\,v^2 \\
&- 18\,u^3\,v + 9\,u^4\Big)\,G(1-v,u)\,\zeta_2 \\
&+ \frac{1}{24\,u^2\,(1-u)^2}\Big(22 - 44\,v + 22\,v^2 - 50\,u + 106\,u\,v - 56\,u\,v^2 + 31\,u^2 - 68\,u^2\,v + 40\,u^2\,v^2 \\
&+ 6\,u^3\,v - 3\,u^4\Big)\Big[G(1,1-v,u)\,H(0,v) - G(1,u)\,H(1,0,v)\Big] \\
&- \frac{1}{24\,u^2\,(1-u)^2}\Big(67 - 134\,v + 67\,v^2 - 128\,u + 250\,u\,v - 122\,u\,v^2 + 58\,u^2 - 110\,u^2\,v + 49\,u^2\,v^2 \\
&- 6\,u^3\,v + 3\,u^4\Big)\,G(1,u)\,\zeta_2 \\
&+ \frac{1}{144\,u^2\,(1-u)^2}\Big(277 - 554\,v + 277\,v^2 - 650\,u + 1264\,u\,v - 614\,u\,v^2 + 430\,u^2 - 770\,u^2\,v \\
&+ 340\,u^2\,v^2 - 18\,u^3 + 60\,u^3\,v - 39\,u^4\Big)\Big[G(1,1-v,u) + G(1,u)\,i\,\pi - G(1,u)\,H(0,v) \\
&- G(1,u)\,H(1,v)\Big] \\
&+ \frac{1}{144\,u^2\,(1-u)^2}\Big(277 - 554\,v + 277\,v^2 - 518\,u + 922\,u\,v - 404\,u\,v^2 + 232\,u^2 - 296\,u^2\,v \\
&+ 25\,u^2\,v^2 - 18\,u^3 - 72\,u^3\,v + 27\,u^4\Big)\,G(1-v,u)\,H(0,v)\,,
\end{aligned}
$$

$$
\begin{aligned}
A_\alpha^{(3)} = \frac{(1-u-v)}{(1-v)}\Bigg[&- \frac{5}{12}\,\zeta_2 - \frac{11}{16}\,i\,\pi\,\zeta_2 - \frac{11}{16}\,H(0,v)\,\zeta_2 + \frac{49}{32}\,\zeta_4 + \frac{7}{4}\,i\,\pi\,\zeta_3 + \frac{7}{4}\,H(0,v)\,\zeta_3 + \frac{389}{144}\,\zeta_3 \\
&- \frac{2759}{864}\,i\,\pi - \frac{2759}{864}\,H(0,v) - \frac{81659}{10368}\Bigg],
\end{aligned}
$$

$$
A_\alpha^{(4)} = 0. \tag{B.1}
$$

$$
\begin{aligned}
A_\beta^{(1)} = \frac{1}{4}\Big[& - G(-v,1-v,-v,u)\,i\,\pi + G(-v,1-v,-v,u)\,H(0,v) - G(-v,1-v,-v,0,u) \\
& - G(-v,1-v,u)\,\zeta_2 - G(-v,1-v,u)\,H(0,v)\,i\,\pi + G(-v,1-v,u)\,H(0,0,v) \\
& - G(-v,1-v,u)\,H(1,0,v) - G(-v,1-v,0,u)\,H(0,v) - 2\,G(-v,-v,-v,u)\,i\,\pi \\
& + 2\,G(-v,-v,-v,u)\,H(0,v) - 2\,G(-v,-v,-v,0,u) - 4\,G(-v,-v,u)\,\zeta_2 \\
& - 2\,G(-v,-v,u)\,H(0,v)\,i\,\pi + 2\,G(-v,-v,u)\,H(0,0,v) + 2\,G(-v,-v,0,u)\,i\,\pi \\
& - 2\,G(-v,-v,0,u)\,H(0,v) + 2\,G(-v,-v,0,0,u) - 2\,G(-v,u)\,\zeta_3 - G(-v,u)\,i\,\pi\,\zeta_2 \\
& - 3\,G(-v,u)\,H(0,0,v)\,i\,\pi + 3\,G(-v,u)\,H(0,0,0,v) - G(-v,u)\,H(0,1,0,v) + G(-v,u)\,H(1,v)\,\zeta_2 \\
& + G(-v,u)\,H(1,0,v)\,i\,\pi - G(-v,u)\,H(1,0,0,v) + G(-v,u)\,H(1,1,0,v) \\
& + 3\,G(-v,0,-v,u)\,i\,\pi - 3\,G(-v,0,-v,u)\,H(0,v) + 3\,G(-v,0,-v,0,u) - G(-v,0,u)\,\zeta_2 \\
& + 2\,G(-v,0,u)\,H(0,v)\,i\,\pi - 3\,G(-v,0,u)\,H(0,0,v) + G(-v,0,u)\,H(1,0,v) \\
& + 2\,G(-v,0,0,u)\,H(0,v) + 2\,G(0,1-v,-v,u)\,i\,\pi - 2\,G(0,1-v,-v,u)\,H(0,v) \\
& + 2\,G(0,1-v,-v,0,u) + 2\,G(0,1-v,u)\,\zeta_2 + 2\,G(0,1-v,u)\,H(0,v)\,i\,\pi \\
& - 2\,G(0,1-v,u)\,H(0,0,v) + 2\,G(0,1-v,u)\,H(1,0,v) + 2\,G(0,1-v,0,u)\,H(0,v) \\
& + 2\,G(0,-v,-v,u)\,i\,\pi - 2\,G(0,-v,-v,u)\,H(0,v) + 2\,G(0,-v,-v,0,u) - 2\,G(0,-v,u)\,\zeta_2 \\
& + G(0,-v,u)\,H(0,v)\,i\,\pi - 2\,G(0,-v,u)\,H(0,0,v) + G(0,-v,0,u)\,H(0,v) - G(0,u)\,H(0,v)\,\zeta_2 \\
& + 2\,G(0,u)\,H(0,0,v)\,i\,\pi - 3\,G(0,u)\,H(0,0,0,v) + G(0,u)\,H(0,1,0,v) \\
& + 2\,G(0,u)\,H(1,0,0,v) - 2\,G(0,0,-v,u)\,i\,\pi + 2\,G(0,0,-v,u)\,H(0,v) \\
& - 2\,G(0,0,-v,0,u) + 2\,G(0,0,u)\,H(0,0,v) - H(0,v)\,i\,\pi\,\zeta_2 \\
& - 3\,H(0,0,0,v)\,i\,\pi + 3\,H(0,0,0,0,v) - H(0,0,1,0,v) + H(0,1,v)\,\zeta_2 \\
& + H(0,1,0,v)\,i\,\pi - H(0,1,0,0,v) + H(0,1,1,0,v) + 2\,H(1,v)\,\zeta_3 + 2\,H(1,0,v)\,\zeta_2 \\
& + 2\,H(1,0,0,v)\,i\,\pi - 2\,H(1,0,0,0,v) + 2\,H(1,0,1,0,v) + 2\,H(1,1,0,0,v)\Big] \\
& + \frac{11}{12}\Big[- G(-v,-v,u)\,i\,\pi + G(-v,-v,u)\,H(0,v) - G(-v,-v,0,u) - G(-v,u)\,H(0,0,v) \\
& + G(-v,0,u)\,H(0,v) - G(-v,0,0,u) - G(0,0,u)\,H(0,v)\Big] \\
& + \frac{39}{32}\,\zeta_4 + \frac{5}{4}\Big[- G(-v,u)\,H(0,v)\,\zeta_2 + H(0,v)\,\zeta_3 - H(0,0,v)\,\zeta_2\Big] + \frac{7}{4}\,i\,\pi\,\zeta_3 - \frac{11}{6}\,G(-v,u)\,\zeta_2 \\
& + \frac{v}{8\,u\,(1-u)^2\,(1-v)^2}\Big(2 - 4\,v + 2\,v^2 - 8\,u + 13\,u\,v - 5\,u\,v^2 + 12\,u^2 - 16\,u^2\,v + 5\,u^2\,v^2 \\
& - 5\,u^3 + 3\,u^3\,v + u^4\Big)\Big[- G(0,-v,u)\,i\,\pi + G(0,-v,u)\,H(0,v) - G(0,-v,0,u)\Big] \\
& + \frac{(1-u)}{4\,u^2}\Big(1 - v + u\Big)\Big[G(1-v,1-v,-v,u)\,i\,\pi - G(1-v,1-v,-v,u)\,H(0,v) \\
& + G(1-v,1-v,-v,0,u) + G(1-v,1-v,u)\,\zeta_2 + G(1-v,1-v,u)\,H(0,v)\,i\,\pi \\
& - G(1-v,1-v,u)\,H(0,0,v) + G(1-v,1-v,u)\,H(1,0,v) + G(1-v,1-v,0,u)\,H(0,v) \\
& + G(1-v,u)\,\zeta_3 + G(1-v,u)\,H(0,v)\,\zeta_2 + G(1-v,u)\,H(0,0,v)\,i\,\pi - G(1-v,u)\,H(0,0,0,v) \\
& + G(1-v,u)\,H(0,1,0,v) + G(1-v,u)\,H(1,0,0,v) - G(1-v,0,-v,u)\,i\,\pi \\
& + G(1-v,0,-v,u)\,H(0,v) - G(1-v,0,-v,0,u) + G(1-v,0,u)\,H(0,0,v) \\
& + G(1,1-v,-v,u)\,i\,\pi - G(1,1-v,-v,u)\,H(0,v) + G(1,1-v,-v,0,u) + G(1,1-v,u)\,\zeta_2 \\
& + G(1,1-v,u)\,H(0,v)\,i\,\pi - G(1,1-v,u)\,H(0,0,v) + G(1,1-v,u)\,H(1,0,v) \\
& + G(1,1-v,0,u)\,H(0,v) + G(1,u)\,\zeta_3 - 2\,G(1,u)\,i\,\pi\,\zeta_2 - G(1,u)\,H(0,v)\,\zeta_2
\end{aligned}
$$

$$
- G(1,u)\,H(0,0,v)\,i\,\pi + G(1,u)\,H(0,0,0,v) - G(1,u)\,H(0,1,0,v) - G(1,u)\,H(1,v)\,\zeta_2
$$
$$
- G(1,u)\,H(1,0,v)\,i\,\pi + G(1,u)\,H(1,0,0,v) - G(1,u)\,H(1,1,0,v) + G(1,0,-v,u)\,i\,\pi
$$
$$
- G(1,0,-v,u)\,H(0,v) + G(1,0,-v,0,u) - 2\,G(1,0,u)\,\zeta_2 - G(1,0,u)\,H(0,0,v)
$$
$$
- G(1,0,u)\,H(1,0,v)\Big]
$$
$$
- \frac{1}{48\,(1-v)\,(u+v)^2}\Big(3\,v - 19\,v^2 + 16\,v^3 - 17\,u\,v + 36\,u\,v^2 - u^2 + 39\,u^2\,v + 19\,u^3\Big)\,G(0,u)
$$
$$
+ \frac{1}{864\,(1-v)\,(u+v)^2}\Big(-54\,v - 2813\,v^2 + 2867\,v^3 - 6004\,u\,v + 6058\,u\,v^2 - 3137\,u^2
$$
$$
+ 3245\,u^2\,v + 54\,u^3\Big)\,i\,\pi
$$
$$
+ \frac{1}{864\,(1-v)^2\,(u+v)^2}\Big(54\,v - 3533\,v^2 + 4537\,v^3 - 1058\,v^4 - 6580\,u\,v + 8822\,u\,v^2
$$
$$
- 1753\,u\,v^3 - 3155\,u^2 + 4735\,u^2\,v - 602\,u^2\,v^2 + 396\,u^3 + 93\,u^3\,v\Big)\,H(0,v)
$$
$$
+ \frac{1}{144\,(1-u)\,(1-v)^2\,(1-u-v)}\Big(295 - 912\,v + 939\,v^2 - 322\,v^3 - 626\,u + 1700\,u\,v
$$
$$
- 1432\,u\,v^2 + 358\,u\,v^3 + 313\,u^2 - 761\,u^2\,v + 421\,u^2\,v^2 + 18\,u^3 + 9\,u^3\,v\Big)\,H(0,v)\,i\,\pi
$$
$$
+ \frac{1}{144\,(1-u)\,(1-v)^2\,(1-u-v)}\Big(295 - 714\,v + 543\,v^2 - 124\,v^3 - 626\,u + 1238\,u\,v
$$
$$
- 772\,u\,v^2 + 160\,u\,v^3 + 313\,u^2 - 431\,u^2\,v + 157\,u^2\,v^2 + 18\,u^3 - 57\,u^3\,v\Big)\,G(0,u)\,H(0,v)
$$
$$
+ \frac{1}{10368\,u\,(1-v)\,(u+v)}\Big(-5184\,v + 5184\,v^2 - 5832\,u - 79967\,u\,v + 85799\,u\,v^2
$$
$$
- 85799\,u^2 + 95771\,u^2\,v + 9972\,u^3\Big)
$$
$$
+ \frac{1}{144\,u\,(1-u)\,(1-v)\,(1-u-v)}\Big(36\,v - 72\,v^2 + 36\,v^3 + 295\,u - 644\,u\,v + 421\,u\,v^2
$$
$$
- 72\,u\,v^3 - 626\,u^2 + 957\,u^2\,v - 349\,u^2\,v^2 + 313\,u^3 - 313\,u^3\,v + 18\,u^4\Big)\,\Big[G(-v,u)\,i\,\pi
$$
$$
- G(-v,u)\,H(0,v) + G(-v,0,u)\Big]
$$
$$
+ \frac{1}{144\,u\,(1-u)\,(1-v)^2\,(1-u-v)}\Big(36 - 144\,v + 216\,v^2 - 144\,v^3 + 36\,v^4 + 187\,u - 318\,u\,v
$$
$$
+ 3\,u\,v^2 + 200\,u\,v^3 - 72\,u\,v^4 - 518\,u^2 + 914\,u^2\,v - 448\,u^2\,v^2 + 52\,u^2\,v^3 + 277\,u^3 - 359\,u^3\,v
$$
$$
+ 121\,u^3\,v^2 + 18\,u^4 - 57\,u^4\,v\Big)\,H(1,0,v)
$$
$$
+ \frac{1}{144\,u\,(1-u)\,(1-v)^2\,(1-u-v)}\Big(72 - 288\,v + 432\,v^2 - 288\,v^3 + 72\,v^4 + 19\,u + 258\,u\,v
$$
$$
- 717\,u\,v^2 + 584\,u\,v^3 - 144\,u\,v^4 - 290\,u^2 + 290\,u^2\,v + 116\,u^2\,v^2 - 116\,u^2\,v^3 + 181\,u^3
$$
$$
- 167\,u^3\,v + 25\,u^3\,v^2 + 18\,u^4 - 57\,u^4\,v\Big)\,\zeta_2
$$
$$
+ \frac{1}{144\,u\,(1-u)\,(1-v)^2\,(1-u-v)}\Big(-36\,v + 108\,v^2 - 108\,v^3 + 36\,v^4 - 295\,u + 543\,u\,v
$$
$$
- 273\,u\,v^2 + 97\,u\,v^3 - 72\,u\,v^4 + 626\,u^2 - 659\,u^2\,v - 14\,u^2\,v^2 + 47\,u^2\,v^3 - 313\,u^3 - 34\,u^3\,v
$$
$$
+ 215\,u^3\,v^2 - 18\,u^4 + 150\,u^4\,v\Big)\,H(0,0,v)
$$
$$
- \frac{1}{8\,u\,(1-u)^2}\Big(2 - 2\,v - 3\,u + 5\,u\,v - 5\,u^2\,v + u^3\Big)\,H(1,0,v)\,i\,\pi
$$

$$
\begin{aligned}
&- \frac{1}{12\,u\,(1-u)^2}\left(6-6\,v+2\,u+15\,u\,v-22\,u^2-15\,u^2\,v+14\,u^3\right) G(0,u)\,\zeta_2\\
&- \frac{1}{16\,u\,(1-u)^2}\left(8-8\,v-u+20\,u\,v-22\,u^2-20\,u^2\,v+15\,u^3\right) i\,\pi\,\zeta_2\\
&+ \frac{1}{24\,u\,(1-u)^2}\left(6-6\,v+13\,u+15\,u\,v-44\,u^2-15\,u^2\,v+25\,u^3\right)\Big[-G(0,u)\,H(1,0,v)\\
&- H(1,v)\,\zeta_2 - H(1,1,0,v)\Big]\\
&+ \frac{1}{8\,u\,(1-u)^2\,(1-v)^2}\left(4-10\,v+8\,v^2-2\,v^3-6\,u+14\,u\,v-13\,u\,v^2+5\,u\,v^3+2\,u^2\,v\right.\\
&\left.+ 4\,u^2\,v^2-5\,u^2\,v^3+2\,u^3-9\,u^3\,v+5\,u^3\,v^2+u^4\,v\right)\Big[G(1-v,-v,u)\,i\,\pi\\
&- G(1-v,-v,u)\,H(0,v)+G(1-v,-v,0,u)+G(1-v,u)\,\zeta_2+G(1-v,u)\,H(0,v)\,i\,\pi\\
&- G(1-v,u)\,H(0,0,v)+G(1-v,u)\,H(1,0,v)+G(1-v,0,u)\,H(0,v)\Big]\\
&+ \frac{1}{24\,u\,(1-u)^2\,(1-v)^2}\left(12-30\,v+24\,v^2-6\,v^3+26\,u-46\,u\,v+5\,u\,v^2+15\,u\,v^3-88\,u^2\right.\\
&\left.+ 182\,u^2\,v-76\,u^2\,v^2-15\,u^2\,v^3+50\,u^3-115\,u^3\,v+59\,u^3\,v^2+3\,u^4\,v\right) H(1,0,0,v)\\
&+ \frac{1}{24\,u\,(1-u)^2\,(1-v)^2}\left(6\,v-12\,v^2+6\,v^3+22\,u-68\,u\,v+61\,u\,v^2-15\,u\,v^3-44\,u^2\right.\\
&\left.+ 124\,u^2\,v-92\,u^2\,v^2+15\,u^2\,v^3+22\,u^3-59\,u^3\,v+31\,u^3\,v^2+3\,u^4\,v\right)\Big[H(0,0,v)\,i\,\pi\\
&+ H(0,1,0,v)\Big]\\
&+ \frac{1}{24\,u\,(1-u)^2\,(1-v)^2}\left(6\,v-12\,v^2+6\,v^3+44\,u-112\,u\,v+83\,u\,v^2-15\,u\,v^3-88\,u^2\right.\\
&\left.+ 212\,u^2\,v-136\,u^2\,v^2+15\,u^2\,v^3+44\,u^3-103\,u^3\,v+53\,u^3\,v^2+3\,u^4\,v\right)\Big[G(0,u)\,H(0,0,v)\\
&- H(0,0,0,v)\Big]\\
&+ \frac{1}{48\,u\,(1-u)^2\,(1-v)^2}\left(12\,v-24\,v^2+12\,v^3-77\,u+106\,u\,v+u\,v^2-30\,u\,v^3+154\,u^2\right.\\
&\left.- 236\,u^2\,v+58\,u^2\,v^2+30\,u^2\,v^3-77\,u^3+124\,u^3\,v-59\,u^3\,v^2+6\,u^4\,v\right) H(0,v)\,\zeta_2\\
&+ \frac{1}{144\,u\,(1-u)^2\,(1-v)^2}\left(72-180\,v+144\,v^2-36\,v^3+413\,u-790\,u\,v+287\,u\,v^2+90\,u\,v^3\right.\\
&\left.- 1042\,u^2+2120\,u^2\,v-970\,u^2\,v^2-90\,u^2\,v^3+557\,u^3-1204\,u^3\,v+611\,u^3\,v^2+18\,u^4\,v\right)\zeta_3,
\end{aligned}
$$

$$
\begin{aligned}
A_\beta^{(2)} = &\frac{11\,v}{12\,u\,(1-u)\,(1-v)^2}\left(2-4\,v+2\,v^2+3\,u\,v-3\,u\,v^2-2\,u^2+3\,u^2\,v-u^3\right) H(0,0,v)\\
&+ \frac{1}{288\,u\,(1-v)}\left(144-144\,v+133\,u-133\,u\,v+277\,u^2\right)\\
&+ \frac{1}{8\,u\,(1-u)}\left(2-2\,v-u+3\,u\,v-u^2\right)\Big[-3\,\zeta_3 - i\,\pi\,\zeta_2 - G(1-v,u)\,H(1,0,v)\\
&+ 4\,H(1,v)\,\zeta_2 + H(1,0,v)\,i\,\pi - H(1,0,1,v) + H(1,1,0,v)\Big]\\
&+ \frac{1}{16\,u\,(1-u)}\left(6-6\,v-3\,u+5\,u\,v-3\,u^2\right)\Big[G(1-v,u)\,i\,\pi - H(1,v)\,i\,\pi\Big]
\end{aligned}
$$

$$
- \frac{1}{24\,u\,(1-u)}\,\Big(22-22\,v-11\,u+39\,u\,v-11\,u^2\Big)\,H(1,0,v)
$$
$$
+ \frac{1}{48\,u\,(1-u)}\,\Big(26-26\,v-13\,u+51\,u\,v-13\,u^2\Big)\,\Big[-G(1-v,1-v,u)
$$
$$
+ G(1-v,u)\,H(1,v)-H(1,1,v)\Big]
$$
$$
+ \frac{1}{288\,u\,(1-u)\,(1-v)}\,\Big(554-1108\,v+554\,v^2-397\,u+1306\,u\,v-909\,u\,v^2-271\,u^2
$$
$$
+ 157\,u^2\,v+114\,u^3\Big)\,\Big[G(1-v,u)-H(1,v)\Big]
$$
$$
+ \frac{1}{288\,u\,(1-u)\,(1-v)}\,\Big(554-1108\,v+554\,v^2-265\,u+1174\,u\,v-909\,u\,v^2-271\,u^2
$$
$$
+ 289\,u^2\,v-18\,u^3\Big)\,i\,\pi
$$
$$
+ \frac{1}{8\,u\,(1-u)\,(1-v)^2}\,\Big(2-10\,v+14\,v^2-6\,v^3-u+8\,u\,v-16\,u\,v^2+9\,u\,v^3-u^2+4\,u^2\,v
$$
$$
- 4\,u^2\,v^2+u^3\,v\Big)\,\Big[G(1-v,1,1-v,u)+G(1-v,1,u)\,i\,\pi-G(1-v,1,u)\,H(0,v)
$$
$$
- G(1-v,1,u)\,H(1,v)\Big]
$$
$$
+ \frac{1}{8\,u\,(1-u)\,(1-v)^2}\,\Big(2-2\,v-2\,v^2+2\,v^3-u+2\,u\,v+2\,u\,v^2-3\,u\,v^3-u^2+2\,u^2\,v^2
$$
$$
- u^3\,v\Big)\,\Big[G(0,1-v,u)\,H(0,v)+G(0,1,1-v,u)+G(0,1,u)\,i\,\pi-G(0,1,u)\,H(0,v)
$$
$$
- G(0,1,u)\,H(1,v)\Big]
$$
$$
- \frac{1}{48\,u\,(1-u)\,(1-v)^2}\,\Big(44-158\,v+184\,v^2-70\,v^3-22\,u+110\,u\,v-193\,u\,v^2+105\,u\,v^3
$$
$$
- 22\,u^2+70\,u^2\,v-61\,u^2\,v^2+13\,u^3\,v\Big)\,H(0,1,v)
$$
$$
+ \frac{1}{48\,u\,(1-u)\,(1-v)^2}\,\Big(44-114\,v+96\,v^2-26\,v^3-22\,u+110\,u\,v-127\,u\,v^2+39\,u\,v^3
$$
$$
- 22\,u^2+26\,u^2\,v+5\,u^2\,v^2-9\,u^3\,v\Big)\,H(0,v)\,i\,\pi
$$
$$
- \frac{1}{48\,u\,(1-u)\,(1-v)^2}\,\Big(160-454\,v+428\,v^2-134\,v^3-80\,u+388\,u\,v-497\,u\,v^2
$$
$$
+ 189\,u\,v^3-80\,u^2+134\,u^2\,v-41\,u^2\,v^2-13\,u^3\,v\Big)\,\zeta_2
$$
$$
- \frac{1}{288\,u\,(1-u)\,(1-v)^2}\,\Big(-554\,v+1108\,v^2-554\,v^3-132\,u+384\,u\,v-1161\,u\,v^2
$$
$$
+ 909\,u\,v^3+494\,u^2\,v-657\,u^2\,v^2+132\,u^3+31\,u^3\,v\Big)\,H(0,v)
$$
$$
+ \frac{1}{4\,u^2}\,\Big(1-v+u\,v\Big)\,\Big[\frac{13}{6}\,G(1,u)\,H(0,v)\,i\,\pi-\frac{35}{6}\,G(1,u)\,H(0,1,v)+\frac{22}{3}\,G(1-v,u)\,H(0,0,v)
$$
$$
- \frac{22}{3}\,G(1,u)\,H(0,0,v)+2\,G(1-v,1-v,u)\,\zeta_2+2\,G(1-v,1-v,u)\,H(0,v)\,i\,\pi
$$
$$
- 2\,G(1-v,1-v,u)\,H(0,1,v)-2\,G(1-v,1-v,1,1-v,u)
$$
$$
- 2\,G(1-v,1-v,1,u)\,i\,\pi+2\,G(1-v,1-v,1,u)\,H(0,v)+2\,G(1-v,1-v,1,u)\,H(1,v)
$$
$$
+ 2\,G(1-v,0,1-v,u)\,H(0,v)+2\,G(1-v,0,1,1-v,u)+2\,G(1-v,0,1,u)\,i\,\pi
$$
$$
- 2\,G(1-v,0,1,u)\,H(0,v)-2\,G(1-v,0,1,u)\,H(1,v)+G(1-v,1,1-v,u)\,H(0,v)
$$
$$
- 4\,G(1-v,1,u)\,\zeta_2-G(1-v,1,u)\,H(0,v)\,i\,\pi+G(1-v,1,u)\,H(0,1,v)
$$

$$
- G(1-v,1,u)\,H(1,0,v) + 2\,G(1-v,1,1,1-v,u) + 2\,G(1-v,1,1,u)\,i\,\pi
$$
$$
- 2\,G(1-v,1,1,u)\,H(0,v) - 2\,G(1-v,1,1,u)\,H(1,v) + 2\,G(1,1-v,1-v,u)\,H(0,v)
$$
$$
- 4\,G(1,1-v,u)\,\zeta_2 - G(1,1-v,u)\,H(0,v)\,i\,\pi + G(1,1-v,u)\,H(0,1,v)
$$
$$
- G(1,1-v,u)\,H(1,0,v) + 3\,G(1,1-v,1,1-v,u) + 3\,G(1,1-v,1,u)\,i\,\pi
$$
$$
- 3\,G(1,1-v,1,u)\,H(0,v) - 3\,G(1,1-v,1,u)\,H(1,v) - 3\,G(1,u)\,\zeta_3 - G(1,u)\,i\,\pi\,\zeta_2
$$
$$
+ 4\,G(1,u)\,H(1,v)\,\zeta_2 + G(1,u)\,H(1,0,v)\,i\,\pi - G(1,u)\,H(1,0,1,v)
$$
$$
+ G(1,u)\,H(1,1,0,v) - G(1,0,1-v,u)\,H(0,v) - G(1,0,1,1-v,u) - G(1,0,1,u)\,i\,\pi
$$
$$
+ G(1,0,1,u)\,H(0,v) + G(1,0,1,u)\,H(1,v) + 2\,G(1,1,1-v,1-v,u)
$$
$$
+ 2\,G(1,1,1-v,u)\,i\,\pi - 2\,G(1,1,1-v,u)\,H(0,v) - 2\,G(1,1,1-v,u)\,H(1,v) - 2\,G(1,1,u)\,\zeta_2
$$
$$
- 2\,G(1,1,u)\,H(1,v)\,i\,\pi + 2\,G(1,1,u)\,H(1,0,v) + 2\,G(1,1,u)\,H(1,1,v)
$$
$$
- 2\,G(1,1,1,1-v,u) - 2\,G(1,1,1,u)\,i\,\pi + 2\,G(1,1,1,u)\,H(0,v) + 2\,G(1,1,1,u)\,H(1,v)\Big]
$$
$$
+ \frac{1}{8\,u^2\,(1-u)}\left(3 - 3\,v - u + 2\,u\,v - u^2 + 3\,u^2\,v - u^3\right)\Big[G(1,1-v,u)\,i\,\pi - G(1,u)\,H(1,v)\,i\,\pi\Big]
$$
$$
+ \frac{1}{24\,u^2\,(1-u)}\left(13 - 13\,v - 19\,u + 38\,u\,v + 3\,u^2 - 31\,u^2\,v + 3\,u^3\right)\Big[
$$
$$
- G(1-v,1-v,u)\,H(0,v) - G(1,1-v,1-v,u) + G(1,1-v,u)\,H(1,v) - G(1,u)\,H(1,1,v)\Big]
$$
$$
+ \frac{1}{24\,u^2\,(1-u)}\left(13 - 13\,v - 7\,u + 14\,u\,v - 3\,u^2 + 5\,u^2\,v - 3\,u^3\right)\Big[- G(1,1,1-v,u)
$$
$$
- G(1,1,u)\,i\,\pi + G(1,1,u)\,H(0,v) + G(1,1,u)\,H(1,v)\Big]
$$
$$
+ \frac{1}{24\,u^2\,(1-u)}\left(22 - 22\,v - 28\,u + 56\,u\,v + 3\,u^2 - 40\,u^2\,v + 3\,u^3\right)\Big[G(1,1-v,u)\,H(0,v)
$$
$$
- G(1,u)\,H(1,0,v)\Big]
$$
$$
- \frac{1}{24\,u^2\,(1-u)}\left(67 - 67\,v - 61\,u + 122\,u\,v - 3\,u^2 - 49\,u^2\,v - 3\,u^3\right)G(1,u)\,\zeta_2
$$
$$
+ \frac{1}{144\,u^2\,(1-u)\,(1-v)}\Big(277 - 554\,v + 277\,v^2 - 355\,u + 969\,u\,v - 614\,u\,v^2 + 21\,u^2
$$
$$
- 379\,u^2\,v + 340\,u^2\,v^2 + 75\,u^3 - 39\,u^3\,v - 18\,u^4\Big)\Big[G(1,1-v,u) + G(1,u)\,i\,\pi
$$
$$
- G(1,u)\,H(0,v) - G(1,u)\,H(1,v)\Big]
$$
$$
+ \frac{1}{8\,u^2\,(1-u)\,(1-v)^2}\Big(3 - 9\,v + 9\,v^2 - 3\,v^3 - 3\,u + 14\,u\,v - 19\,u\,v^2 + 8\,u\,v^3 - 3\,u^2\,v
$$
$$
+ 9\,u^2\,v^2 - 6\,u^2\,v^3 - 2\,u^3\,v + 3\,u^3\,v^2 - u^4\,v\Big)\,G(1-v,u)\,H(0,v)\,i\,\pi
$$
$$
+ \frac{1}{24\,u^2\,(1-u)\,(1-v)^2}\Big(13 - 39\,v + 39\,v^2 - 13\,v^3 - 13\,u + 46\,u\,v - 53\,u\,v^2 + 20\,u\,v^3
$$
$$
- 13\,u^2\,v + 17\,u^2\,v^2 - 4\,u^2\,v^3 + 6\,u^3\,v - 9\,u^3\,v^2 + 3\,u^4\,v\Big)\,G(1-v,u)\,H(0,1,v)
$$
$$
- \frac{1}{24\,u^2\,(1-u)\,(1-v)^2}\Big(13 - 39\,v + 39\,v^2 - 13\,v^3 + 5\,u - 8\,u\,v + u\,v^2 + 2\,u\,v^3 - 9\,u^2
$$
$$
+ 32\,u^2\,v - 46\,u^2\,v^2 + 23\,u^2\,v^3 - 9\,u^3 + 24\,u^3\,v - 18\,u^3\,v^2 + 3\,u^4\,v\Big)\,G(1-v,u)\,\zeta_2
$$
$$
+ \frac{1}{144\,u^2\,(1-u)\,(1-v)^2}\Big(277 - 831\,v + 831\,v^2 - 277\,v^3 - 223\,u + 850\,u\,v - 1031\,u\,v^2
$$
$$
+ 404\,u\,v^3 - 45\,u^2 - 70\,u^2\,v + 140\,u^2\,v^2 - 25\,u^2\,v^3 + 9\,u^3 + 96\,u^3\,v - 144\,u^3\,v^2 - 18\,u^4
$$

$$+ 57\,u^4\,v\Big)\,G(1-v,u)\,H(0,v)\,,$$

$$A_\beta^{(3)} = \frac{u}{(1-v)}\Bigg[+\frac{5}{12}\,\zeta_2 + \frac{11}{16}\,i\,\pi\,\zeta_2 + \frac{11}{16}\,H(0,v)\,\zeta_2 - \frac{49}{32}\,\zeta_4 - \frac{7}{4}\,i\,\pi\,\zeta_3 - \frac{7}{4}\,H(0,v)\,\zeta_3 - \frac{389}{144}\,\zeta_3$$
$$+ \frac{2759}{864}\,i\,\pi + \frac{2759}{864}\,H(0,v) + \frac{81659}{10368}\Bigg]\,,$$

$$A_\beta^{(4)} = 0\,, \tag{B.2}$$

$$A_\gamma^{(1)} = \frac{v\,(1-u-v)}{8\,u\,(1-u)^3}\Big(2-5\,u+5\,u^2\Big)\Big[-2\,i\,\pi\,\zeta_2 - 2\,G(0,u)\,\zeta_2 - G(0,u)\,H(1,0,v)$$
$$- H(1,v)\,\zeta_2 - H(1,0,v)\,i\,\pi - H(1,1,0,v)\Big]$$
$$+ \frac{v\,(1-u-v)}{4\,u^2}\Big[G(1-v,1-v,-v,u)\,i\,\pi - G(1-v,1-v,-v,u)\,H(0,v)$$
$$+ G(1-v,1-v,-v,0,u) + G(1-v,1-v,u)\,\zeta_2 + G(1-v,1-v,u)\,H(0,v)\,i\,\pi$$
$$- G(1-v,1-v,u)\,H(0,0,v) + G(1-v,1-v,u)\,H(1,0,v) + G(1-v,1-v,0,u)\,H(0,v)$$
$$+ G(1-v,u)\,\zeta_3 + G(1-v,u)\,H(0,v)\,\zeta_2 + G(1-v,u)\,H(0,0,v)\,i\,\pi$$
$$- G(1-v,u)\,H(0,0,0,v) + G(1-v,u)\,H(0,1,0,v) + G(1-v,u)\,H(1,0,0,v)$$
$$- G(1-v,0,-v,u)\,i\,\pi + G(1-v,0,-v,u)\,H(0,v) - G(1-v,0,-v,0,u)$$
$$+ G(1-v,0,u)\,H(0,0,v) + G(1,1-v,-v,u)\,i\,\pi - G(1,1-v,-v,u)\,H(0,v)$$
$$+ G(1,1-v,-v,0,u) + G(1,1-v,u)\,\zeta_2 + G(1,1-v,u)\,H(0,v)\,i\,\pi$$
$$- G(1,1-v,u)\,H(0,0,v) + G(1,1-v,u)\,H(1,0,v) + G(1,1-v,0,u)\,H(0,v)$$
$$+ G(1,u)\,\zeta_3 - 2\,G(1,u)\,i\,\pi\,\zeta_2 - G(1,u)\,H(0,v)\,\zeta_2 - G(1,u)\,H(0,0,v)\,i\,\pi$$
$$+ G(1,u)\,H(0,0,0,v) - G(1,u)\,H(0,1,0,v) - G(1,u)\,H(1,v)\,\zeta_2 - G(1,u)\,H(1,0,v)\,i\,\pi$$
$$+ G(1,u)\,H(1,0,0,v) - G(1,u)\,H(1,1,0,v) + G(1,0,-v,u)\,i\,\pi - G(1,0,-v,u)\,H(0,v)$$
$$+ G(1,0,-v,0,u) - 2\,G(1,0,u)\,\zeta_2 - G(1,0,u)\,H(0,0,v) - G(1,0,u)\,H(1,0,v)\Big]$$
$$+ \frac{v}{8\,u\,(1-u)^3\,(1-v)^2}\Big(4-10\,v+8\,v^2-2\,v^3-12\,u+30\,u\,v-23\,u\,v^2+5\,u\,v^3+12\,u^2$$
$$- 34\,u^2\,v + 26\,u^2\,v^2 - 5\,u^2\,v^3 - u^3 + 11\,u^3\,v - 7\,u^3\,v^2 - 4\,u^4 + u^4\,v + u^5\Big)\Big[\zeta_3$$
$$+ G(1-v,-v,u)\,i\,\pi - G(1-v,-v,u)\,H(0,v) + G(1-v,-v,0,u) + G(1-v,u)\,\zeta_2$$
$$+ G(1-v,u)\,H(0,v)\,i\,\pi - G(1-v,u)\,H(0,0,v) + G(1-v,u)\,H(1,0,v)$$
$$+ G(1-v,0,u)\,H(0,v) + H(1,0,0,v)\Big]$$
$$+ \frac{v}{8\,u\,(1-u)^3\,(1-v)^2}\Big(2\,v-4\,v^2+2\,v^3+2\,u-8\,u\,v+11\,u\,v^2-5\,u\,v^3-8\,u^2+16\,u^2\,v$$
$$- 14\,u^2\,v^2 + 5\,u^2\,v^3 + 9\,u^3 - 9\,u^3\,v + 3\,u^3\,v^2 - 4\,u^4 + u^4\,v + u^5\Big)\Big[-G(0,-v,u)\,i\,\pi$$
$$+ G(0,-v,u)\,H(0,v) - G(0,-v,0,u) + G(0,u)\,H(0,0,v) + H(0,v)\,\zeta_2 + H(0,0,v)\,i\,\pi$$
$$- H(0,0,0,v) + H(0,1,0,v)\Big]$$
$$+ \frac{(1-u-v)}{288\,(1-v)^2}\Big(132+31\,v\Big)\,H(0,v) + \frac{(1-u-v)}{16\,(1-u)\,(1-v)}\Big(3-2\,v-u\Big)\,i\,\pi$$

$$
\begin{aligned}
&- \frac{(1-u-v)}{48\,(1-u)\,(1-v)} \Big(13 + 6\,v - 19\,u\Big)\, G(0,u) \\
&+ \frac{1}{16\,(1-u)^2\,(1-v)^2} \Big(2 + 3\,v - 7\,v^2 + 2\,v^3 - 4\,u - 13\,u\,v + 20\,u\,v^2 - 6\,u\,v^3 + 4\,u^2 + 7\,u^2\,v \\
&- 5\,u^2\,v^2 - 2\,u^3 - u^3\,v\Big)\, H(0,v)\, i\,\pi \\
&+ \frac{1}{48\,(1-u)^2\,(1-v)^2} \Big(6 - 13\,v + v^2 + 6\,v^3 - 12\,u + 27\,u\,v + 16\,u\,v^2 - 18\,u\,v^3 + 12\,u^2 \\
&- 45\,u^2\,v + 7\,u^2\,v^2 - 6\,u^3 + 19\,u^3\,v\Big)\, G(0,u)\, H(0,v) \\
&- \frac{1}{288\,u\,(1-v)} \Big(144\,v - 144\,v^2 - 133\,u + 133\,u\,v + 277\,u^2\Big) \\
&+ \frac{1}{8\,u\,(1-u)^2\,(1-v)} \Big(-2\,v^2 + 2\,v^3 - u - u\,v + 7\,u\,v^2 - 4\,u\,v^3 + 2\,u^2 + 2\,u^2\,v - 5\,u^2\,v^2 \\
&- 2\,u^3 + u^3\,v + u^4\Big) \Big[-G(-v,u)\, i\,\pi + G(-v,u)\, H(0,v) - G(-v,0,u)\Big] \\
&- \frac{1}{24\,u\,(1-u)^2\,(1-v)^2} \Big(6\,v^2 - 12\,v^3 + 6\,v^4 + 3\,u - 22\,u\,v - 2\,u\,v^2 + 33\,u\,v^3 - 12\,u\,v^4 - 6\,u^2 \\
&+ 66\,u^2\,v - 23\,u^2\,v^2 - 15\,u^2\,v^3 + 6\,u^3 - 75\,u^3\,v + 25\,u^3\,v^2 - 3\,u^4 + 25\,u^4\,v\Big)\, H(0,0,v) \\
&+ \frac{1}{48\,u\,(1-u)^2\,(1-v)^2} \Big(12\,v - 36\,v^2 + 36\,v^3 - 12\,v^4 + 6\,u - 49\,u\,v + 97\,u\,v^2 - 78\,u\,v^3 + 24\,u\,v^4 \\
&- 12\,u^2 + 51\,u^2\,v - 32\,u^2\,v^2 + 6\,u^2\,v^3 + 12\,u^3 - 45\,u^3\,v + 7\,u^3\,v^2 - 6\,u^4 + 19\,u^4\,v\Big)\, H(1,0,v) \\
&+ \frac{1}{48\,u\,(1-u)^2\,(1-v)^2} \Big(24\,v - 72\,v^2 + 72\,v^3 - 24\,v^4 + 6\,u - 85\,u\,v + 193\,u\,v^2 - 162\,u\,v^3 \\
&+ 48\,u\,v^4 - 12\,u^2 + 75\,u^2\,v - 80\,u^2\,v^2 + 30\,u^2\,v^3 + 12\,u^3 - 45\,u^3\,v + 7\,u^3\,v^2 - 6\,u^4 + 19\,u^4\,v\Big)\, \zeta_2\,,
\end{aligned}
$$

$$
\begin{aligned}
A_\gamma^{(2)} = {}& \frac{v\,(1-u-v)}{8\,u\,(1-u)^2} \Big(2 - 3\,u\Big) \Big[-3\,\zeta_3 - i\,\pi\,\zeta_2 - G(1-v,u)\, H(1,0,v) + 4\,H(1,v)\,\zeta_2 \\
&+ H(1,0,v)\, i\,\pi - H(1,0,1,v) + H(1,1,0,v)\Big] \\
&+ \frac{v\,(1-u-v)}{16\,u\,(1-u)^2} \Big(6 - 5\,u\Big) \Big[G(1-v,u)\, i\,\pi - H(1,v)\, i\,\pi\Big] \\
&- \frac{v\,(1-u-v)}{24\,u\,(1-u)^2} \Big(22 - 39\,u\Big)\, H(1,0,v) \\
&+ \frac{v\,(1-u-v)}{48\,u\,(1-u)^2} \Big(26 - 51\,u\Big) \Big[-G(1-v,1-v,u) + G(1-v,u)\, H(1,v) - H(1,1,v)\Big] \\
&+ \frac{v\,(1-u-v)}{8\,u\,(1-u)^2\,(1-v)^2} \Big(4 - 10\,v + 6\,v^2 - 6\,u + 14\,u\,v - 9\,u\,v^2 + 2\,u^2\,v - u^3\Big) \\
&\times \Big[G(1-v,1,1-v,u) + G(1-v,1,u)\, i\,\pi - G(1-v,1,u)\, H(0,v) - G(1-v,1,u)\, H(1,v)\Big] \\
&+ \frac{v\,(1-u-v)}{8\,u\,(1-u)^2\,(1-v)^2} \Big(2\,v - 2\,v^2 - 2\,u\,v + 3\,u\,v^2 - 2\,u^2\,v + u^3\Big) \Big[\frac{22}{3}\, H(0,0,v) \\
&+ G(0,1-v,u)\, H(0,v) + G(0,1,1-v,u) + G(0,1,u)\, i\,\pi - G(0,1,u)\, H(0,v) \\
&- G(0,1,u)\, H(1,v)\Big]
\end{aligned}
$$

$$
+ \frac{v\,(1-u-v)}{48\,u\,(1-u)^2\,(1-v)^2}\,\Big(44 - 114\,v + 70\,v^2 - 66\,u + 158\,u\,v - 105\,u\,v^2 + 26\,u^2\,v - 13\,u^3\Big)
\times\Big[- H(0,1,v)\Big]
+ \frac{v\,(1-u-v)}{48\,u\,(1-u)^2\,(1-v)^2}\,\Big(44 - 70\,v + 26\,v^2 - 66\,u + 114\,u\,v - 39\,u\,v^2 - 18\,u^2\,v
+ 9\,u^3\Big)\,H(0,v)\,i\,\pi
- \frac{v\,(1-u-v)}{48\,u\,(1-u)^2\,(1-v)^2}\,\Big(160 - 294\,v + 134\,v^2 - 228\,u + 430\,u\,v - 189\,u\,v^2 - 26\,u^2\,v + 13\,u^3\Big)\,\zeta_2
+ \frac{v\,(1-u-v)}{4\,u^2}\,\Big[\frac{13}{6}\,G(1,u)\,H(0,v)\,i\,\pi - \frac{35}{6}\,G(1,u)\,H(0,1,v) + \frac{22}{3}\,G(1-v,u)\,H(0,0,v)
- \frac{22}{3}\,G(1,u)\,H(0,0,v) + 2\,G(1-v,1-v,u)\,\zeta_2 + 2\,G(1-v,1-v,u)\,H(0,v)\,i\,\pi
- 2\,G(1-v,1-v,u)\,H(0,1,v) - 2\,G(1-v,1-v,1,1-v,u) - 2\,G(1-v,1-v,1,u)\,i\,\pi
+ 2\,G(1-v,1-v,1,u)\,H(0,v) + 2\,G(1-v,1-v,1,u)\,H(1,v) + 2\,G(1-v,0,1-v,u)\,H(0,v)
+ 2\,G(1-v,0,1,1-v,u) + 2\,G(1-v,0,1,u)\,i\,\pi - 2\,G(1-v,0,1,u)\,H(0,v)
- 2\,G(1-v,0,1,u)\,H(1,v) + G(1-v,1,1-v,u)\,H(0,v) - 4\,G(1-v,1,u)\,\zeta_2
- G(1-v,1,u)\,H(0,v)\,i\,\pi + G(1-v,1,u)\,H(0,1,v) - G(1-v,1,u)\,H(1,0,v)
+ 2\,G(1-v,1,1,1-v,u) + 2\,G(1-v,1,1,u)\,i\,\pi - 2\,G(1-v,1,1,u)\,H(0,v)
- 2\,G(1-v,1,1,u)\,H(1,v) + 2\,G(1,1-v,1-v,u)\,H(0,v) - 4\,G(1,1-v,u)\,\zeta_2
- G(1,1-v,u)\,H(0,v)\,i\,\pi + G(1,1-v,u)\,H(0,1,v) - G(1,1-v,u)\,H(1,0,v)
+ 3\,G(1,1-v,1,1-v,u) + 3\,G(1,1-v,1,u)\,i\,\pi - 3\,G(1,1-v,1,u)\,H(0,v)
- 3\,G(1,1-v,1,u)\,H(1,v) - 3\,G(1,u)\,\zeta_3 - G(1,u)\,i\,\pi\,\zeta_2 + 4\,G(1,u)\,H(1,v)\,\zeta_2
+ G(1,u)\,H(1,0,v)\,i\,\pi - G(1,u)\,H(1,0,1,v) + G(1,u)\,H(1,1,0,v)
- G(1,0,1-v,u)\,H(0,v) - G(1,0,1,1-v,u) - G(1,0,1,u)\,i\,\pi + G(1,0,1,u)\,H(0,v)
+ G(1,0,1,u)\,H(1,v) + 2\,G(1,1,1-v,1-v,u) + 2\,G(1,1,1-v,u)\,i\,\pi
- 2\,G(1,1,1-v,u)\,H(0,v) - 2\,G(1,1,1-v,u)\,H(1,v) - 2\,G(1,1,u)\,\zeta_2
- 2\,G(1,1,u)\,H(1,v)\,i\,\pi + 2\,G(1,1,u)\,H(1,0,v) + 2\,G(1,1,u)\,H(1,1,v)
- 2\,G(1,1,1,1-v,u) - 2\,G(1,1,1,u)\,i\,\pi + 2\,G(1,1,1,u)\,H(0,v) + 2\,G(1,1,1,u)\,H(1,v)\Big]
+ \frac{v\,(1-u-v)}{8\,u^2\,(1-u)^2}\,\Big(3 - 2\,u - 3\,u^2\Big)\,\Big[G(1,1-v,u)\,i\,\pi - G(1,u)\,H(1,v)\,i\,\pi\Big]
+ \frac{v\,(1-u-v)}{12\,u^2\,(1-u)^2}\,\Big(11 - 28\,u + 20\,u^2\Big)\,\Big[G(1,1-v,u)\,H(0,v) - G(1,u)\,H(1,0,v)\Big]
+ \frac{v\,(1-u-v)}{24\,u^2\,(1-u)^2}\,\Big(13 - 38\,u + 31\,u^2\Big)\,\Big[- G(1-v,1-v,u)\,H(0,v) - G(1,1-v,1-v,u)
+ G(1,1-v,u)\,H(1,v) - G(1,u)\,H(1,1,v)\Big]
+ \frac{v\,(1-u-v)}{24\,u^2\,(1-u)^2}\,\Big(13 - 14\,u - 5\,u^2\Big)\,\Big[- G(1,1,1-v,u) - G(1,1,u)\,i\,\pi + G(1,1,u)\,H(0,v)
+ G(1,1,u)\,H(1,v)\Big]
- \frac{v\,(1-u-v)}{24\,u^2\,(1-u)^2}\,\Big(67 - 122\,u + 49\,u^2\Big)\,G(1,u)\,\zeta_2
$$

$$
\begin{aligned}
&+\frac{v\,(1-u-v)}{8\,u^2\,(1-u)^2\,(1-v)^2}\,\Big(3-6\,v+3\,v^2-6\,u+14\,u\,v-8\,u\,v^2+3\,u^2-8\,u^2\,v+6\,u^2\,v^2\\
&-2\,u^3\,v+u^4\Big)\,G(1-v,u)\,H(0,v)\,i\,\pi\\
&+\frac{v\,(1-u-v)}{24\,u^2\,(1-u)^2\,(1-v)^2}\,\Big(13-26\,v+13\,v^2-26\,u+46\,u\,v-20\,u\,v^2+13\,u^2-20\,u^2\,v\\
&+4\,u^2\,v^2+6\,u^3\,v-3\,u^4\Big)\,G(1-v,u)\,H(0,1,v)\\
&-\frac{v\,(1-u-v)}{24\,u^2\,(1-u)^2\,(1-v)^2}\,\Big(13-26\,v+13\,v^2-8\,u+10\,u\,v-2\,u\,v^2-14\,u^2+34\,u^2\,v\\
&-23\,u^2\,v^2+6\,u^3\,v-3\,u^4\Big)\,G(1-v,u)\,\zeta_2\\
&+\frac{(1-u-v)}{288\,u\,(1-u)^2\,(1-v)}\,\Big(-554\,v+554\,v^2+36\,u+987\,u\,v-909\,u\,v^2-150\,u^2-78\,u^2\,v\\
&+114\,u^3\Big)\,\Big[-G(1-v,u)+H(1,v)\Big]\\
&+\frac{(1-u-v)}{288\,u\,(1-u)^2\,(1-v)}\,\Big(554\,v-554\,v^2-36\,u-855\,u\,v+909\,u\,v^2+18\,u^2-54\,u^2\,v+18\,u^3\Big)\,i\,\pi\\
&+\frac{(1-u-v)}{288\,u\,(1-u)^2\,(1-v)^2}\,\Big(554\,v^2-554\,v^3+96\,u\,v-842\,u\,v^2+909\,u\,v^3-132\,u^2+228\,u^2\,v\\
&-422\,u^2\,v^2+132\,u^3+31\,u^3\,v\Big)\,H(0,v)\\
&+\frac{(1-u-v)}{144\,u^2\,(1-u)^2\,(1-v)}\,\Big(277\,v-277\,v^2-18\,u-614\,u\,v+614\,u\,v^2+36\,u^2+358\,u^2\,v\\
&-340\,u^2\,v^2-36\,u^3-18\,u^3\,v+18\,u^4\Big)\,\Big[G(1,1-v,u)+G(1,u)\,i\,\pi-G(1,u)\,H(0,v)\\
&-G(1,u)\,H(1,v)\Big]\\
&+\frac{(1-u-v)}{144\,u^2\,(1-u)^2\,(1-v)^2}\,\Big(-277\,v+554\,v^2-277\,v^3+18\,u+464\,u\,v-886\,u\,v^2+404\,u\,v^3\\
&-36\,u^2-124\,u^2\,v+224\,u^2\,v^2-25\,u^2\,v^3+36\,u^3-18\,u^3\,v-96\,u^3\,v^2-18\,u^4+57\,u^4\,v\Big)\\
&\times\Big[-G(1-v,u)\,H(0,v)\Big]\\
&+\frac{1}{288\,u\,(1-u)\,(1-v)}\,\Big(144\,v-144\,v^2+144\,u-11\,u\,v-133\,u\,v^2-421\,u^2+144\,u^2\,v+277\,u^3\Big)\,,
\end{aligned}
$$

$$
A_\gamma^{(3)}=0\,,
$$

$$
A_\gamma^{(4)}=0\,. \tag{B.3}
$$

C. Helicity amplitudes for $q\bar{q}\to Vg$ and $qg\to Vq$

In [21] the helicity amplitudes for the processes

$$
\gamma^*(p_4)\longrightarrow q(p_1)+\bar{q}(p_2)+g(p_3) \tag{C.1}
$$

have been computed. As already discussed, the kinematical region relevant for 3-jet production is characterised by q^2 and s_{ij} all positive.

Following [24], we can analytically continue these matrix elements to the kinematical configuration relevant for $(V+1j)$ production at hadron colliders, which is the same kinematical situation relevant for the $V\gamma$ production studied above:

$$q(p_2)+\bar{q}(p_1)\longrightarrow g(-p_3)+\gamma^*(p_4)\,, \tag{C.2}$$

and

$$q(p_2)+g(p_3)\longrightarrow q(-p_1)+\gamma^*(p_4)\,, \tag{C.3}$$

The kinematical situation in (C.2) is the same as for,

$$q(p_2)+\bar{q}(p_1)\longrightarrow \gamma(-p_3)+V(p_4)\,, \tag{C.4}$$

so we can introduce again the dimensionless variables

$$u=-\frac{s_{13}}{s_{12}}=-\frac{y}{x}\,,\qquad v=\frac{q^2}{s_{12}}=\frac{1}{x}\,, \tag{C.5}$$

which fulfil

$$0\le u\le v\,,\qquad 0\le v\le 1\,.$$

On the other hand, the kinematical situation in (C.3) can be described with the following choice of dimensionless variables [24]:

$$u'=-\frac{s_{13}}{s_{23}}=-\frac{y}{z}\,,\qquad v'=\frac{q^2}{s_{23}}=\frac{1}{z}\,, \tag{C.6}$$

which fulfil again:

$$0\le u'\le v'\,,\qquad 0\le v'\le 1\,.$$

The helicity amplitude coefficients α, β and γ are vectors in colour space and have perturbative expansions:

$$\Omega=\sqrt{4\pi\alpha}\sqrt{4\pi\alpha_s}\,\boldsymbol{T}^a_{ij}\,\left[\Omega^{(0)}+\left(\frac{\alpha_s}{2\pi}\right)\Omega^{(1)}+\left(\frac{\alpha_s}{2\pi}\right)^2\Omega^{(2)}+\mathcal{O}(\alpha_s^3)\right]\,,$$

for $\Omega=\alpha,\beta,\gamma$. The dependence on (u,v) or (u',v') is again implicit.

The ultraviolet and infrared properties of the helicity coefficients are fully described in [21],

$$\begin{aligned}
\Omega^{(0)} &= \Omega^{(0),\mathrm{un}},\\
\Omega^{(1)} &= S_\epsilon^{-1}\Omega^{(1),\mathrm{un}}-\frac{\beta_0}{2\epsilon}\Omega^{(0),\mathrm{un}},\\
\Omega^{(2)} &= S_\epsilon^{-2}\Omega^{(2),\mathrm{un}}-\frac{3\beta_0}{2\epsilon}S_\epsilon^{-1}\Omega^{(1),\mathrm{un}}-\left(\frac{\beta_1}{4\epsilon}-\frac{3\beta_0^2}{8\epsilon^2}\right)\Omega^{(0),\mathrm{un}},
\end{aligned} \tag{C.7}$$

and

$$\begin{aligned}
\Omega^{(1)} &= \boldsymbol{I}^{(1)}(\epsilon)\Omega^{(0)}+\Omega^{(1),\mathrm{finite}},\\
\Omega^{(2)} &= \left(-\frac{1}{2}\boldsymbol{I}^{(1)}(\epsilon)\boldsymbol{I}^{(1)}(\epsilon)-\frac{\beta_0}{\epsilon}\boldsymbol{I}^{(1)}(\epsilon)+e^{-\epsilon\gamma}\frac{\Gamma(1-2\epsilon)}{\Gamma(1-\epsilon)}\left(\frac{\beta_0}{\epsilon}+K\right)\boldsymbol{I}^{(1)}(2\epsilon)+\boldsymbol{H}^{(2)}(\epsilon)\right)\Omega^{(0)}
\end{aligned}$$

$$+\boldsymbol{I}^{(1)}(\epsilon)\Omega^{(1)} + \Omega^{(2),\text{finite}}, \tag{C.8}$$

where the infrared singularity operator $\boldsymbol{I}^{(1)}(\epsilon)$ is a 1×1 matrix in colour space and is given by

$$\boldsymbol{I}^{(1)}(\epsilon) = -\frac{e^{\epsilon\gamma}}{2\Gamma(1-\epsilon)}\left[N\left(\frac{1}{\epsilon^2}+\frac{3}{4\epsilon}+\frac{\beta_0}{2N\epsilon}\right)(\mathtt{S}_{13}+\mathtt{S}_{23}) - \frac{1}{N}\left(\frac{1}{\epsilon^2}+\frac{3}{2\epsilon}\right)\mathtt{S}_{12}\right], \tag{C.9}$$

where (since we have set $\mu^2 = s_{123}$)

$$\mathtt{S}_{ij} = \left(-\frac{s_{123}}{s_{ij}}\right)^{\epsilon}. \tag{C.10}$$

Expanding $\mathtt{S}_{ij}$, imaginary parts are generated, the sign of which is fixed by the small imaginary part $+i0$ of s_{ij}.
Finally we have

$$\boldsymbol{H}^{(2)}(\epsilon) = \frac{e^{\epsilon\gamma}}{4\,\epsilon\,\Gamma(1-\epsilon)}H^{(2)}\ , \tag{C.11}$$

where, in the $\overline{\text{MS}}$ scheme:

$$\begin{aligned} H^{(2)} = &\left(4\zeta_3 + \frac{589}{432} - \frac{11\pi^2}{72}\right)N^2 + \left(-\frac{1}{2}\zeta_3 - \frac{41}{54} - \frac{\pi^2}{48}\right) + \left(-3\zeta_3 - \frac{3}{16} + \frac{\pi^2}{4}\right)\frac{1}{N^2} \\ &+ \left(-\frac{19}{18} + \frac{\pi^2}{36}\right)NN_F + \left(-\frac{1}{54} - \frac{\pi^2}{24}\right)\frac{N_F}{N} + \frac{5}{27}N_F^2. \end{aligned} \tag{C.12}$$

They finite one-loop amplitudes can be decomposed according to their colour structure as follows:

$$\Omega^{(1),\text{finite}}(u,v) = N\,a_\Omega(u,v) + \frac{1}{N}\,b_\Omega(u,v) + \beta_0\,c_\Omega(u,v)\ . \tag{C.13}$$

We attach to the arXiv submission of the paper the one loop coefficients expanded up to $\mathcal{O}(\epsilon^2)$.

The finite two-loop remainder is obtained by subtracting the predicted infrared structure (expanded through to $\mathcal{O}(\epsilon^0)$) from the renormalised helicity coefficient. We further decompose the finite remainder according to the colour structure, as follows:

$$\begin{aligned} \Omega^{(2),\text{finite}}(u,v) = &N^2 A_\Omega(u,v) + B_\Omega(u,v) + \frac{1}{N^2}C_\Omega(u,v) + NN_F D_\Omega(u,v) \\ &+ \frac{N_F}{N}E_\Omega(u,v) + N_F^2 F_\Omega(u,v) + N_{F,V}\left(\frac{4}{N} - N\right)G_\Omega(u,v)\ , \end{aligned}$$

The complete expressions in FORM format can be found attached to the arXiv submission of this paper.

References

[1] U. Baur, E. L. Berger, Phys. Rev. **D41** (1990) 1476; Phys. Rev. **D47** (1993) 4889.

[2] L. J. Dixon, Z. Kunszt, A. Signer, Phys. Rev. **D60** (1999) 114037 [hep-ph/9907305].

[3] V. M. Abazov *et al.* [D0 Collaboration], Phys. Rev. **D71** (2005) 091108 [hep-ex/0503048]; Phys. Lett. **B653** (2007) 378 [arXiv:0705.1550]; Phys. Rev. Lett. **100** (2008) 241805 [arXiv:0803.0030]; Phys. Rev. Lett. **102** (2009) 201802 [arXiv:0902.2157];
D. Acosta *et al.* [CDF II Collaboration], Phys. Rev. Lett. **94** (2005) 041803. [hep-ex/0410008];
T. Aaltonen *et al.* [CDF Collaboration], Phys. Rev. **D82** (2010) 031103. [arXiv:1004.1140].

[4] S. Chatrchyan *et al.* [CMS Collaboration], Phys. Lett. **B701** (2011) 535 [arXiv:1105.2758]; G. Aad *et al.* [ATLAS Collaboration], JHEP **1109** (2011) 072 [arXiv:1106.1592].

[5] J. Ohnemus, Phys. Rev. **D47** (1993) 940;
U. Baur, T. Han, J. Ohnemus, Phys. Rev. **D48** (1993) 5140 [hep-ph/9305314]; Phys. Rev. **D57** (1998) 2823 [hep-ph/9710416].

[6] L. J. Dixon, Z. Kunszt and A. Signer, Nucl. Phys. B **531** (1998) 3 [hep-ph/9803250].

[7] E. Accomando, A. Denner, C. Meier, Eur. Phys. J. **C47** (2006) 125 [hep-ph/0509234].

[8] V. Del Duca, F. Maltoni, Z. Nagy, Z. Trocsanyi, JHEP **0304** (2003) 059 [hep-ph/0303012].

[9] F. Campanario, C. Englert, M. Spannowsky, D. Zeppenfeld, Europhys. Lett. **88** (2009) 11001 [arXiv:0908.1638];
F. Campanario, C. Englert, M. Spannowsky, Phys. Rev. **D83** (2011) 074009 [arXiv:1010.1291].

[10] S. Dittmaier, S. Kallweit, P. Uwer, Phys. Rev. Lett. **100** (2008) 062003 [arXiv:0710.1577]; Nucl. Phys. **B826** (2010) 18 [arXiv:0908.4124];
J. M. Campbell, R. K. Ellis, G. Zanderighi, JHEP **0712** (2007) 056. [arXiv:0710.1832];
T. Binoth, T. Gleisberg, S. Karg, N. Kauer, G. Sanguinetti, Phys. Lett. **B683** (2010) 154 [arXiv:0911.3181];
F. Campanario, C. Englert, S. Kallweit, M. Spannowsky, D. Zeppenfeld, JHEP **1007** (2010) 076 [arXiv:1006.0390].

[11] T. Binoth and G. Heinrich, Nucl. Phys. B **585** (2000) 741 [hep-ph/0004013], Nucl. Phys. B **693** (2004) 134 [hep-ph/0402265];
C. Anastasiou, K. Melnikov and F. Petriello, Phys. Rev. D **69** (2004) 076010 [hep-ph/0311311];
G. Heinrich, Int. J. Mod. Phys. A **23** (2008) 1457 [arXiv:0803.4177];
J. Carter and G. Heinrich, Comput. Phys. Commun. **182** (2011) 1566 [arXiv:1011.5493];
C. Anastasiou, F. Herzog and A. Lazopoulos, JHEP **1103** (2011) 038. [arXiv:1011.4867], [arXiv:1110.2368].

[12] S. Catani, M. Grazzini, Phys. Rev. Lett. **98** (2007) 222002. [hep-ph/0703012].

[13] A. Gehrmann-De Ridder, T. Gehrmann, E. W. N. Glover, JHEP **0509** (2005) 056 [hep-ph/0505111];
A. Gehrmann-De Ridder, T. Gehrmann, E. W. N. Glover, G. Heinrich, JHEP **0711** (2007) 058 [arXiv:0710.0346].

[14] A. Daleo, T. Gehrmann, D. Maitre, JHEP **0704** (2007) 016 [hep-ph/0612257];
A. Daleo, A. Gehrmann-De Ridder, T. Gehrmann, G. Luisoni, JHEP **1001** (2010) 118 [arXiv:0912.0374];
R. Boughezal, A. Gehrmann-De Ridder, M. Ritzmann, JHEP **1102** (2011) 098 [arXiv:1011.6631];
T. Gehrmann, P. F. Monni, [arXiv:1107.4037].

[15] E. W. N. Glover, J. Pires, JHEP **1006** (2010) 096 [arXiv:1003.2824].

[16] S. Catani, L. Cieri, D. de Florian, G. Ferrera, M. Grazzini, [arXiv:1110.2375].

[17] C. Anastasiou, E. W. N. Glover, M. E. Tejeda-Yeomans, Nucl. Phys. **B629** (2002) 255 [hep-ph/0201274].

[18] Z. Bern, A. De Freitas, L. J. Dixon, JHEP **0109** (2001) 037 [hep-ph/0109078].

[19] G. Chachamis, M. Czakon, D. Eiras, JHEP **0812** (2008) 003 [arXiv:0802.4028].

[20] L. W. Garland, T. Gehrmann, E. W. N. Glover, A. Koukoutsakis and E. Remiddi, Nucl. Phys. B **627** (2002) 107 [hep-ph/0112081].

[21] L. W. Garland, T. Gehrmann, E. W. N. Glover, A. Koukoutsakis and E. Remiddi, Nucl. Phys. B **642** (2002) 227 [hep-ph/0206067].

[22] A. Gehrmann-De Ridder, T. Gehrmann, E.W.N. Glover and G. Heinrich, Phys. Rev. Lett. **99** (2007) 132002 [arXiv:0707.1285]; JHEP **0712** (2007) 094 [arXiv:0711.4711]; Phys. Rev. Lett. **100** (2008) 172001 [arXiv:0802.0813]; JHEP **0905** (2009) 106 [arXiv:0903.4658].

[23] S. Weinzierl, Phys. Rev. Lett. **101** (2008) 162001 [arXiv:0807.3241]; JHEP **0906** (2009) 041 [arXiv:0904.1077]; JHEP **0907** (2009) 009 [arXiv:0904.1145]; Phys. Rev. D **80** (2009) 094018 [arXiv:0909.5056]. Eur. Phys. J. C **71** (2011) 1565 [arXiv:1011.6247].

[24] T. Gehrmann and E. Remiddi, Nucl. Phys. B **640** (2002) 379 [hep-ph/0207020].

[25] L. J. Dixon, Proceedings of TASI'94 "QCD & Beyond", ed. D. Soper, World Scientific, 1995, p. 539 [hep-ph/9601359].

[26] P. Nogueira, J. Comput. Phys. **105** (1993) 279.

[27] S. Moch, J. A. M. Vermaseren and A. Vogt, Phys. Lett. B **625** (2005) 245 [hep-ph/0508055].

[28] P. A. Baikov, K. G. Chetyrkin, A. V. Smirnov, V. A. Smirnov, M. Steinhauser, Phys. Rev. Lett. **102** (2009) 212002 [arXiv:0902.3519];
R. N. Lee, A. V. Smirnov, V. A. Smirnov, JHEP **1004** (2010) 020 [arXiv:1001.2887];
T. Gehrmann, E.W.N. Glover, T. Huber, N. Ikizlerli, C. Studerus JHEP **1006** (2010) 094 [arXiv:1004.3653].

[29] F. V. Tkachov, Phys. Lett. B **100** (1981) 65.
K. G. Chetyrkin and F. V. Tkachov, Nucl. Phys. B **192** (1981) 159.

[30] S. Laporta, Int. J. Mod. Phys. A **15** (2000) 5087 [hep-ph/0102033].

[31] C. Studerus, Comput. Phys. Commun. **181** (2010) 1293 [arXiv:0912.2546].

[32] T. Gehrmann and E. Remiddi, Nucl. Phys. **B601** (2001) 248 [hep-ph/0008287]; **B601** (2001) 287 [hep-ph/0101124].

[33] T. Gehrmann and E. Remiddi, Nucl. Phys. **B580** (2000) 485 [hep-ph/9912329].

[34] E. Remiddi and J.A.M. Vermaseren, Int. J. Mod. Phys. **A15** (2000) 725 [hep-ph/9905237].

[35] T. Gehrmann and E. Remiddi, Comput. Phys. Commun. **141** (2001) 296 [hep-ph/0107173]; Comput. Phys. Commun. **144** (2002) 200 [hep-ph/0111255];
J. Vollinga, S. Weinzierl, Comput. Phys. Commun. **167** (2005) 177. [hep-ph/0410259];
D. Maître, Comput. Phys. Commun. **174** (2006) 222 [hep-ph/0507152];
D. Maitre, Comput. Phys. Commun. **183** (2012) 846 [hep-ph/0703052];
S. Bühler, C. Duhr, [arXiv:1106.5739].

[36] J.A.M. Vermaseren, *New features of FORM*, math-ph/0010025; Nucl. Phys. Proc. Suppl. **183** (2008) 19 [arXiv:0806.4080].

[37] S. Catani, Phys. Lett. **B427** (1998) 161 [hep-ph/9802439].

[38] R.K. Ellis, D.A. Ross and A.E. Terrano, Nucl. Phys. B **178** (1981) 421.

[39] W.T. Giele and E.W.N. Glover, Phys. Rev. D **46** (1992) 1980.